DISSERTATIONES
TECHNOLOGIAE
UNIVERSITATIS
TARTUENSIS
56

MEERI VISNAPUU

Design and physico-chemical characterization of metal-containing nanoparticles for antimicrobial coatings

DISSERTATIONES TECHNOLOGIAE UNIVERSITATIS TARTUENSIS
56

MEERI VISNAPUU

Design and physico-chemical characterization of metal-containing nanoparticles for antimicrobial coatings

UNIVERSITY OF TARTU
Press

This study was carried out at the Institute of Physics, Faculty of Science and Technology, University of Tartu in collaboration with the National Institute of Chemical Physics and Biophysics.

This dissertation was accepted for the commencement of the degree of Doctor of Philosophy in Environmental Engineering on November 4th, 2019 by the Council of the Institute of Technology, Faculty of Science and Technology, University of Tartu, Estonia.

Supervisors: Dr Vambola Kisand, Institute of Physics, University of Tartu
Dr Angela Ivask, National Institute of Chemical Physics and Biophysics (until 2018); Ministry of Social Affairs of Estonia (since 2018)

Dr Margit Heinlaan, National Institute of Chemical Physics and Biophysics

Opponent: Dr Maja Dutour Sikirić, Head of the Laboratory for biocolloids and interface chemistry, Division of Physical Chemistry, Ruđer Bošković Institute, Zagreb, Croatia

Defence: Auditorium 121, Nooruse 1, Tartu, Estonia, at 14:15 on December 17th, 2019

This work was financially supported by the following agencies and foundations: Estonian Research Council (Grants ETF8216, PUT748, IUT2-25 and IUT23-5), EU FP7 NanoValid Project (Contract 263147), ERF project Graduate School of functional materials and technologies, European Social Fund's Doctoral Studies and Internationalisation Programme DoRa, Estonian Centre of Excellence in Research Projects "Emerging orders in quantum and nanomaterials (TK134)", "Advanced materials and high-technology devices for sustainable energetics, sensorics and nanoelectronics (TK141)", "High-technology Materials for Sustainable Development" (TK117), "Mesosystems–Theory and Applications" (TK114).

ISSN 2228-0855
ISBN 978-9949-03-232-7 (print)
ISBN 978-9949-03-233-4 (pdf)

University of Tartu Press
www.tyk.ee

CONTENTS

LIST OF PUBLICATIONS

Paper I **M. Visnapuu**, U. Joost, K. Juganson, K. Künnis-Beres, A. Kahru, V. Kisand, A. Ivask, Dissolution of silver nanowires and nanospheres dictates their toxicity to *Escherichia coli*, *BioMed Research International* (2013) 819252.

Paper II A. Ivask, I. Kurvet, K. Kasemets, I. Blinova, V. Aruoja, S. Suppi, H. Vija, A. Käkinen, T. Titma, M. Heinlaan, **M. Visnapuu**, D. Koller, V. Kisand, A. Kahru, Size-dependent toxicity of silver nanoparticles to bacteria, yeast, algae, crustaceans and mammalian cells in vitro, *PLOS ONE* 9 (2014) e102108.

Paper III A. Ivask, **M. Visnapuu**, P. Vallotton, E. R. Marzouk, E. Lombi, N. H. Voelcker, Quantitative multimodal analyses of silver nanoparticle-cell interactions: Implications for cytotoxicity, *NanoImpact* 1 (2016) 29–38.

Paper IV U. Joost, K. Juganson, **M. Visnapuu**, M. Mortimer, A. Kahru, E. Nõmmiste, U. Joost, V. Kisand, A. Ivask, Photocatalytic antibacterial activity of nano-TiO_2 (anatase)-based thin films: Effects on *Escherichia coli* cells and fatty acids, *Journal of Photochemistry and Photobiology B: Biology* 142 (2015) 178–185.

Paper V **M. Visnapuu**, M. Rosenberg, E. Truska, E. Nõmmiste, A. Šutka, A. Kahru, M. Rähn, H. Vija, K. Orupõld, V. Kisand, A. Ivask, UVA-induced antimicrobial activity of ZnO/Ag nano-composite covered surfaces, *Colloids and Surfaces B: Biointerfaces* 169 (2018) 222–232.

AUTHOR'S CONTRIBUTION

Paper I Contribution to the design of the experiments. Conducting the experiments (material characterization; toxicity, bioavailability, viability tests), analysing data. Participating in preparation of the manuscript.

Paper II Performing material characterization experiments (TEM, SEM), analysing data.

Paper III Preparation of cell samples (exposure, chemical etching) for subsequent analysis (ICP-MS, imaging flow cytometry), analysing data.

Paper IV Contribution to the design of the experiments. Conducting the experiments (antibacterial study, SEM imaging), analysing data. Participating in preparation of the manuscript.

Paper V Contribution to the design of the experiments. Conducting the experiments (particle synthesis, surface preparation, photocatalysis study, antimicrobial study), analysing data. Participating in preparation of the manuscript.

OTHER PUBLICATIONS OF THE DISSERTANT

1. A. Šutka, M. Järvekülg, K. A. Gross, M. Kook, T. Käämbre, **M. Visnapuu**, G. Trefalt, A. Šutka, Visible light to switch-on desorption from goethite, *Nanoscale* 11 (2019) 3794–3798.
2. A. Ivask, E. H. Pilkington, T. Blin, A. Käkinen, H. Vija, **M. Visnapuu**, J. F. Quinn, M. R. Whittaker, R. Qiao, T. P. Davis, P.-C. Ke, N. H. Voelcker, Uptake and transcytosis of functionalized superparamagnetic iron oxide nanoparticles in an in vitro blood brain barrier model, *Biomaterials Science* 6 (2018) 314–323.
3. A. Šutka, M. Antsov, M. Järvekülg, **M. Visnapuu**, I. Heinmaa, U. Mäeorg, S. Vlassov, A. Šutka, Mechanical properties of individual fiber segments of electrospun lignocellulose-reinforced poly(vinyl alcohol), *Journal of Applied Polymer Science* 134 (2017) 44361.
4. U. Joost, A. Šutka, **M. Visnapuu**, A. Tamm, M. Lembinen, M. Antsov, K. Utt, K. Smits, E. Nõmmiste, V. Kisand, Colorimetric gas detection by the varying thickness of a thin film of ultrasmall PTSA-coated TiO_2 nanoparticles on a Si substrate, *Beilstein Journal of Nanotechnology* 8 (2017) 229–236.
5. O. M. Bondarenko, A. Ivask, A. Kahru, H. Vija, T. Titma, **M. Visnapuu**, U. Joost, K. Pudova, S. Adamberg, T. Visnapuu, T. Alamäe, Bacterial polysaccharide levan as stabilizing, non-toxic and functional coating material for microelement-nanoparticles, *Carbohydrate Polymers* 136 (2015) 710–720.
6. A. Šutka, M. Timusk, N. Döbelin, R. Pärna, **M. Visnapuu**, U. Joost, T. Käämbre, V. Kisand, K. Saal, M. Knite, A straightforward and "green" solvothermal synthesis of Al doped zinc oxide plasmonic nanocrystals and piezoresistive elastomer nanocomposite, *RSC Advances* 5 (2015) 63846–63852.
7. A. Ivask, T. Titma, **M. Visnapuu**, H. Vija, A. Käkinen, M. Sihtmäe, S. Pokhel, L. Madler, M. Heinlaan, V. Kisand, R. Shimmo, A. Kahru, Toxicity of 11 metal oxide nanoparticles to three mammalian cell types in vitro, *Current Topics in Medicinal Chemistry* 15 (2015), 1914–1929.
8. U. Joost, A. Saarva, **M. Visnapuu**, E. Nõmmiste, K. Utt, R. Saar, V. Kisand, Purification of titania nanoparticle thin films: Triviality or a challenge? *Ceramics International* 40 (2014), 7125–7132.
9. U. Joost, R. Pärna, M. Lembinen, K. Utt, I. Kink, **M. Visnapuu**, V. Kisand, Heat treatment and substrate dependent properties of titania thin films with high copper loading, *Physica Status Solidi A – Applications and Materials Science* 210 (2013) 1201–1212.

ABBREVIATIONS

AAS	atomic absorption spectroscopy
acac	acetylacetone
ATP	adenosine triphosphate
bPEI	branched polyethylenimine
DLS	dynamic light scattering
DNA	deoxyribonucleic acid
EC_{50}	half-effective concentration; the concentration of the test substance that induces the designated effect in 50% of the test organisms after a specified exposure time
EDX	energy dispersive x-ray spectroscopy
EN	European Standard
GSH	glutathione
HCAI	healthcare associated infection
H_2DCFDA	2,7-dichlorodihydrofluorescein diacetate
IC_{50}	half-inhibitory concentration; the concentration of the test substance that inhibits the biological process (e.g. growth, viability) by 50%
ICP-MS	inductively coupled plasma mass spectrometry
ISO	International Organization for Standardization
n.a.	not analysed
n.o.	not observed
NM	nanomaterial
NP	nanoparticle
NS	nanosphere
NW	nanowire
PBS	phosphate-buffered saline
pdi	polydispersity index
PEG	polyethylene glycol
PTSA	*p*-toluenesulfonic acid
ROS	reactive oxygen species
SEM	scanning electron microscopy
SOD	superoxide dismutase
SSC	side scatter
TEM	transmission electron microscopy
$Ti(OBu)_4$	titanium(IV) butoxide
TXRF	total reflection x-ray fluorescence spectroscopy
UVA	ultraviolet A
UVC	ultraviolet C
UV-Vis	ultraviolet–visible
XPS	x-ray photoelectron spectroscopy
XRD	x-ray diffraction

1. INTRODUCTION

The constant need for materials with new or improved functionalities has provoked a wide use of nanotechnology in consumer and industrial product development. Engineered nanomaterials (less than 100 nm in at least one dimension) have unique properties compared to the respective bulk material making them desirable in a wide range of applications.

Many consumer products aim to prevent the spread of microbes. Silver nanoparticles (Ag NPs) are one of the most frequently used nanomaterials (NMs) in consumer products as Ag is known for its antimicrobial properties. Antimicrobial products are meant to kill or inhibit the growth of predominantly bacteria without causing harm to so-called non-target organisms. Therefore, the potential toxic effects of antimicrobial materials, including NPs towards humans as one of the non-target organisms need to be understood to enable their safe implementation. NMs are not considered dangerous per se, but dangers and uncertainties in many aspects regarding their safe use still exist.

Particle physico-chemical properties, such as size, shape and surface properties, as well as the surrounding media, can significantly affect NP influence through altering particle-cell interactions. One of the main toxicity pathways of some NPs, e.g., Ag NPs is their dissolution and release of metal ions. Therefore, dissolution of NPs is a characteristic that needs a special attention in toxicity assessment. Lack of suitable methods for visualization and quantification of NP-cell interactions has not enabled to clarify whether the toxic effects of Ag NPs are caused by cell surface-bound NPs resulting in local dissolution and release of Ag^+ ions or by internalized Ag NPs. Therefore, methods need to be combined to relate cell-particle interactions with cytotoxicity. Understanding of nanoparticle toxic properties allows proceeding with product development without affecting the environment and human health.

A promising perspective for NP use is their application in antimicrobial coatings with the ability to inhibit bacterial growth and even degrade organic residues from the surface. The most often used NPs in such applications are metallic and metal oxide NPs. NPs of Ag and ZnO exhibit their effect through enhanced release of metal ions resulting from the large surface area of the NPs. NPs of metal oxides such as TiO_2 and ZnO are photocatalytically active, i.e., hinder microbe growth and degrade various organic contaminants under specific lighting conditions. Therefore, a formation of nanoparticulate photocatalytic material in combination with antimicrobial metallic NPs would result in a combined effect of antimicrobial ions and photocatalysis.

The purpose of the current study was to gain knowledge on the toxicity of nanosized Ag particles with different physico-chemical properties. The improved knowledge was expected to contribute to the development of novel and sustainable antimicrobial coatings. As a result of the study we propose an antimicrobial coating that is based on a combination of photocatalytic and antimicrobial metallic NPs that enable efficient inhibition of bacterial growth as well as degradation of organic material on surfaces. We also demonstrate the reusability of our coatings which to our best knowledge hasn't been done before for this type of coatings.

2. AIMS OF THE STUDY

The present thesis aims to develop nanoparticle-based antimicrobial coatings that efficiently inhibit the growth of pathogenic bacteria but are safe for human use. The specific aims were:

- to clarify the role of physico-chemical properties (shape, size, surface charge and dissolution) of the most widely used antimicrobial nanoparticles' effects towards model pathogenic bacteria and relevant mammalian cell lines;
- to study the mechanisms behind antimicrobial action of photocatalytically active surfaces;
- to design and propose safe nanoparticle combinations for antimicrobial surface coatings with enhanced photocatalytic and antimicrobial effect.

3. LITERATURE REVIEW

3.1. Advantages and challenges related to nanomaterials

The definition for "nanomaterial" varies slightly in different European Union legislations and is under constant revision[1, 2] but overall, nanomaterials (NMs) are classified on the basis of size and are considered to be materials with at least one dimension in the range of 1–100 nm or particles in agglomerates or aggregates whenever the constituent particles are in the mentioned size range[3]. The current work focuses on particles in nanoscale size range i.e. nanoparticles (NPs). The interest towards nano-scale materials and processes has emerged due to unique physico-chemical properties of NPs that arise mostly due to increased specific surface area compared to the bulk substance. The significantly increased specific surface area of NPs in turn results in increased surface reactivity due to high ratio of surface atoms. Although natural (incl. incidental) nanosized matter has always existed in the environment (e.g. released during combustion processes like volcano eruptions) and surrounded humans, the emergence of nano-technology and engineered NPs has put the environment and humans in a novel situation[4]. Current synthesis methods enable the production of particles with a wide range of physico-chemical properties e.g. size, shape, crystallinity, composition, surface properties. Spherical NPs are most commonly produced and used however, differently shaped particles (nanowires, nanocubes, nanoplates, nanorods etc) have been shown to have great potential in specific applications. For example, Ag or ZnO nanowires could potentially be used in electro-optical applications like solar cells[5–7] and Ag nanoplates show potential as a contrast agent in tumour imaging[8].

NPs find use in various applications due to their enhanced optical, mechanical, electrical, catalytic, biologic etc activity[4]. The properties required for technological applications may lead to increased bioavailability and toxicity of NPs compared to bulk and microsized compounds. Although NMs are not considered dangerous per se, there exist risks regarding their safe use. Consumer products mostly make use of the novel properties of metal-based NPs among which Ag NPs with well-known antimicrobial properties are currently the most used NPs[9]. The data on toxicological impact of NPs are just emerging and still lag behind the design of new NMs[10, 11].

Probably the biggest challenge regards antimicrobial NPs that are meant to be toxic towards microbes per se. These particles however should not affect the non-target cells and organisms. Among the three well-known antimicrobial and biocidal NPs (Ag, ZnO, CuO), Ag NPs have been shown to be the most toxic towards environmentally relevant (non-target) organisms[12], such as environment-inhabiting bacteria and plants, at environmentally relevant concentrations[13]. The estimated annual production of Ag NPs in Europe is ~10 tons[14] and Ag NPs have demonstrated to exhibit toxic effects. Therefore, the need to understand the

magnitude of potential toxicity of nanoscale Ag towards non-target environmental organisms and the human is of great importance. In the following chapters (i) the toxicity pathways of metal-based NPs and (ii) the effect of NP physicochemical properties on their biological activity and NP-cell interactions will be introduced. Ag NPs as the most widely used metal-based NPs will be in the focus.

3.2. Toxicity mechanisms of metal-based nanoparticles

Generally, three major phenomena drive the toxicity of metal-based NPs: (i) release of ions during dissolution of NPs, (ii) organism dependent cellular uptake of NPs and (iii) induction of oxidative stress and the consequent cellular damages[15]. The toxic effect of metal-based CuO, ZnO and Ag NPs has been shown to be mediated by dissolved ions[12]. Also, reactive oxygen species (ROS)-induced oxidative stress and the resulting physiological effects of Ag, ZnO and CuO NPs have been demonstrated at almost all the levels of biological organization, from bacteria to fish as well as in mammalian cell lines *in vitro*[15]. Induction of ROS in addition to ion release is one of the best acknowledged mechanism of toxicity of Ag NPs[16]. However, Ag NPs' toxicity mechanisms in the case of bacteria and mammalian cells are somewhat different.

In the case of bacteria, toxicity of Ag NPs (which is driving also the antibacterial effects of these NPs) is shown to be driven by (i) adherence to the surface of the cell membrane and the following disturbance of membrane permeability and respiration[17], (ii) penetration of the cell membrane and induction of the subsequent physiological effects[18] and (iii) release of silver ions[19–21] (Figure 1).

Adherence of Ag NPs to bacterial membrane has been proven using electron microscopy[18] and atomic force microscopy[22]. Morones et al. 2005 suggest that Ag NPs increase bacterial membrane permeability making it possible for particles to penetrate the cell[19]. Kumar et al. claim cellular uptake of TiO_2 and ZnO NPs by *Salmonella typhimurium* using TEM and flow cytometry analysis[23]. However, for bacteria, internalization of NPs due to rigid cell wall is rather an exception and mostly reported as a side-effect.

Increased adherence enhances Ag bioavailability which leads to increased interference with the normal function of the bacterial electron transport chain and ROS formation at the cell membrane[22]. Bactericidal action of Ag NPs can be attributed to disruptions in ATP generation due to altered respiratory electron transport, increased membrane permeability, inhibition of respiratory chain enzymes and generation of ROS[24]. Increased ROS levels can be the result of disruptions in ROS regulatory pathways[24] as Ag^+ ions released from Ag NPs are proposed to strongly interact with thiol groups of vital enzymes and inactivate them[19]. Also, loss of DNA replication ability and structural changes in the cell membrane have been reported to occur after Ag^+ ion treatment[25]. The importance of Ag^+ ions in Ag NPs toxicity has been proven by the diminished toxicity in anaerobic conditions due to the lack of oxidative dissolution and subsequent ion

release[20]. Lok et al. have as well shown that chemisorbed Ag^+ is the cause for Ag NP antimicrobial activity as reduced Ag NPs (particles without chemisorbed ions) did not cause antibacterial effect[26]. Direct contact between Ag NPs and bacterial cells has proven to be a prerequisite for enhanced Ag NP antibacterial effect due to additional dissolution taking place at particle-cell interface[21].

Antimicrobial effects of NPs can be bacteria-specific due to differences in cell membrane structure. For example, Gram-positive bacteria *Staphylococcus aureus* is shown to be less susceptible to Ag NPs than Gram-negative *Escherichia coli*[27]. Less pronounced changes in cell morphology of *S. aureus* compared to *E. coli* after Ag^+ treatment suggests a defense mechanism of *S. aureus*[25]. However, different susceptibility to Ag NPs has also been observed for bacteria with similar membrane structure, e.g., Gram-negative *Pseudomonas aeruginosa* and *Vibrio cholerae* have been shown to be more resistant to Ag NP toxicity than Gram-negative *E. coli*[19]. Recently, it has been concluded that there is a need to study the bacterial transcriptomic profile in relation to the proteomic profile to comprehensively elucidate the molecular mechanisms behind Ag NP bactericidal action[24].

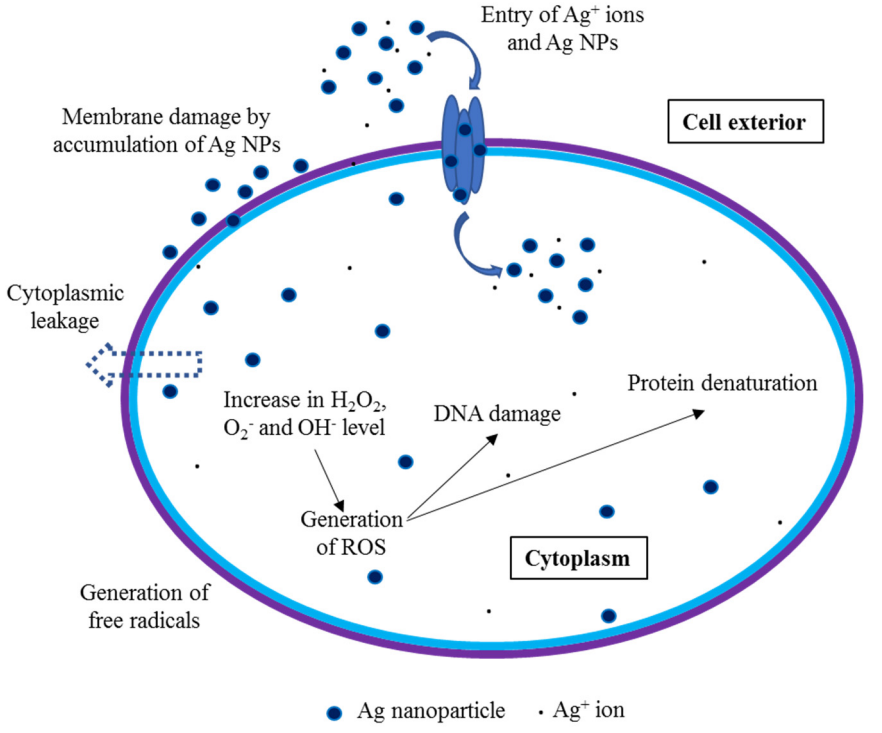

Figure 1. The effects of Ag nanoparticles (NPs) on the bacterial cell. Ag NPs and Ag^+ ions released from the particles can damage bacterial cell membrane and disturb membrane permeability and respiration causing cytoplasmic leakage. Internalized Ag NPs and Ag^+ ions induce increased ROS generation and cause subsequent physiological effects (e.g. DNA damage, protein denaturation). Modified from (Pareek et al. 2018)[24].

In the case of mammalian cells, differently from the bacteria, the uptake of NPs is a very common scenario. Caveolae- and clathrin-mediated endocytosis have been shown to be the main contributors to NP uptake[28, 29]. By using uptake inhibitors it has been suggested that lipid-raft mediated endocytosis, energy-dependent uptake pathways and energy-independent diffusion are all involved in the uptake of Ag NPs[30]. The preferred uptake pathways have been shown to be NP specific and depend on NP parameters such as composition, size, shape and surface chemistry as well as on purity of the particles, incubation conditions and cell types[28]. Particle sizes suitable for uptake range from 10 to 500 nm, but 40–50 nm diameter seems to be the optimal NP size for cellular binding and internalization[31]. The internalized NPs generally translocate to endosomal or lysosomal vesicles for further elimination. Internalized NPs can cause cytotoxicity i.e. toxicity to mammalian cells through the production of ROS and direct mitochondrial damage[31]. The significance of Ag^+ ions in toxicity towards mammalian cells is well-studied. Ag NPs may facilitate the entrance of Ag^+ ions into mammalian cells by so called "Trojan horse" mechanism by which the internalized NPs dissolve and by that, increase the bioavailability of silver[32]. The released Ag^+ ions cause cytotoxicity while intracellular localization of NPs is not that important[32]. A study investigating the fate of intracellular Ag NPs suggested that internalized Ag NPs dissolve quickly and the released ions bind to SH-groups in amino acids or proteins and subsequently affect protein functions and antioxidant defense system of the cells[30] (e.g. the depletion of glutathione (GSH) and reduction of the superoxide dismutase (SOD) enzyme activity). As SODs and GSH-dependent enzymes are the major enzymatic antioxidants in cells[33], depletion of GSH level increases oxidative stress. Increased amount of reactive oxygen radicals stimulated by Ag NPs may be an important factor in their genotoxic effects[30, 34]. Although ROS generation is one of the most frequently reported NP-associated toxicity mechanisms[35], Chairuangkitti et al. have reported both ROS-dependent (cytotoxicity) and ROS-independent (cell cycle arrest) pathways for Ag NP toxicity in A549 cells (human alveolar epithelial cells)[36]. A question concerning metal ion releasing particles is whether the oxidative stress experienced by cells is directly induced by extracellular or internalized NPs, caused by the released ions or a combination of nano-specific NP-cell interactions resulting in increased levels of bioavailable metal ions.

3.3. The effect of nanoparticle physico-chemical properties on their biological activity and nanoparticle-cell interactions

The interactions between NPs and organisms can be complex and vary depending on the characteristics of the particles, types of cells (prokaryotic and eukaryotic) and organisms involved and the properties of the exposure media. Metal-based NP-cell interactions can be roughly classified as (i) adherence to the cell membrane, (ii) penetration of the damaged cell membrane, (iii) internalization by regulated uptake pathways, (iv) extracellular or intracellular release of metal ions and the subsequent interaction with cells.

Physico-chemical properties (size, shape, composition and surface properties such as surface coating) of metal-based NPs may significantly affect particle toxicity through either altered NP-cell interactions or variations in particle dissolution, both of which may increase the bioavailable portion of the metal component of NPs[12, 15, 24, 37]. The extent of NP dissolution is suggested to additionally depend on the properties of the surrounding media. For instance stable colloidal Ag NPs can lead to increased cell-NP association and/or dissolution and consequently to higher toxicity[37]. The importance of proper particle characterization in relevant test conditions has been emphasized[12] and the lack of coherent test conditions and proper characterization may be the reason for controversial data gained by different research groups. The following chapters will describe physico-chemical characterization of NPs and size, shape and surface properties-based biological effects of metal-based NPs on bacterial and mammalian cells with the emphasis on Ag NPs.

3.3.1. Physico-chemical characterization of nanoparticles

A prerequisite for a well-devised and executed study is the appropriate characterization of NPs to make the claims and conclusions of the study[38]. Important aspects of NP characterization can be classified into three main groups: physico-chemical properties, biological and environmental fate, and (re)activity[39]. Physico-chemical properties of NPs can be divided into (i) intrinsic material properties which include chemical composition, size, size distribution, shape, crystal structure, crystallinity and surface characteristics and (ii) extrinsic (altered by the environment) properties which include hydrodynamic diameter, the extent of aggregation or agglomeration, composition of bio-corona, zeta-potential and dissolution[40]. In the case of metal and metal oxide NPs dissolution properties are particularly important to investigate as the release of ionic components must be taken into consideration[41]. Analysis of NPs' extrinsic properties in relevant biological environments poses a challenge due to low realistic NP concentrations and the presence of natural nanoparticulate matter which may complicate analysis[42].

However, knowledge of intrinsic properties or so-called particle synthetic identity may help to predict their biological fate and physiological activity[40].

NPs' properties can be studied using a variety of methods and generally a combination of techniques is used to enable sufficient characterization. Methods for characterization of nanosized matter include electron microscopy (SEM, TEM) and light scattering methods (e.g. DLS) for size, size distribution and aggregation state measurement, spectroscopy methods (e.g. EDX, XPS, UV-Vis) for chemical composition analysis, atomic spectrometry techniques (e.g. AAS, ICP-MS) for elemental analysis and zeta-potential measurement for surface charge and colloidal stability analysis[39, 42]. NPs' inherent reactivity is analysed by measuring their redox potential, radical formation potential and photocatalytic activity[39]. Sample preparation for characterization may alter NP characteristics (e.g. effects from drying in the case of electron microscopy samples or effects from dispersion protocols which affect the degree of particle agglomeration) and that must be taken into consideration when interpreting the results.

It is advisable to characterize several common NP parameters to describe what the particle is made of (chemical composition), what it looks like (size, size distribution, shape) and which factors influence their biological effects (e.g. surface charge, solubility). At the same time, it is important to keep in mind that the choice of the NP characteristics to be measured more accurately should be fit-for-purpose i.e. tailored to the end point being studied[40].

3.3.2. Effects on bacterial cells

As explained in the previous chapter, interaction of dissolved Ag^+ ions from Ag NPs is one of the main cellular interaction mechanisms for Ag NPs, but physico-chemical properties of Ag NPs have been shown to highly influence the type and degree of interactions with bacterial cells[24]. In general, smaller particles tend to induce higher antibacterial activity independent of the NP constituent material[31]. Several studies have concluded that smaller Ag NPs cause higher antimicrobial activity due to increased release of Ag^+ ions[43–45]. Increased dissolution, accompanying decreasing particle size often explains the tendencies observed in antibacterial effect[46]. However, for non-soluble NPs lower antimicrobial effect for smaller NPs[47] or no evident size-dependent toxicity[48] has been published.

It has also been observed that the shape of Ag NPs can impact their antimicrobial activity. Compared to spherical and rod-shaped Ag NPs triangular nanoplates showed higher antibacterial activity[49]. Sadeghi et al. reported that Ag nanoplates had higher antibacterial effect than Ag nanorods with Ag nanospheres being the least effective[50]. Higher area of active crystal facets with high biological reactivity has been claimed to be the cause for increased antimicrobial activity of Ag triangular nanoplates compared to spherical or rod-shaped particles[49, 50]. Namely, the dissolution of Ag from [111] crystal facets (predominant in rod- and plate shaped NPs) is easier which consequently leads to increased Ag^+ release[51]. Controversially in another study, Ag nanoplates were reported to be less

antibacterial than spherical and rod-shaped particles[52]. Shape-dependent toxicity has been shown for other environmentally relevant organisms. Ag nanoplates induced higher toxicity towards zebrafish embryos compared to spherical particles[53]. Shape-dependent antibacterial activity has also been shown for non-soluble materials in which case the adverse effects are not due to chemical (ion-based) but physical reasons. For example rod-shaped carbon structures were reported to puncture bacterial cell membranes[54].

Particle surface can be intentionally functionalized using different ligands. Selection of capping material is relevant as it can significantly affect the dissolution kinetics and release of active silver ions from the surface of Ag NPs[24]. At the same time, in a media containing proteins and other organics, particles tend to spontaneously accumulate an organic surface coating which affects solubility and toxicity of metal NPs[12]. Particle surface properties can also affect cell-NP interactions. Compared to negatively charged particles, positively charged Ag particles have higher adherence affinity for bacterial surface, causing enhanced antibacterial effect[22, 51] due to higher Ag bioavailability[22] and destruction of membrane causing leakage of cellular material[55].

3.3.3. Effects on mammalian cells

As majority of Ag containing consumer products come into contact with humans, toxicity for the human as one of the non-target organisms is studied to evaluate material safety. Ag NP toxicity towards human cells is known from a number of studies[12]. The choice of mammalian cell line for a study depends on the relevant NP exposure scenario. NPs may invade the human body via inhalation, ingestion or through skin and therefore toxic effects towards lung cells, blood cells, epidermis cells etc are studied. The potential use of Ag NPs in drug delivery and targeting[56] has also raised the need to understand Ag NP-cell interactions on tissue cells[29].

Cytotoxicity of NPs has been shown to be particle size dependent. Smaller Ag and Au particles have been shown to induce more significant effects than bigger ones due to increased particle internalization[57], oxidative stress[46], necrosis and apoptosis[58] and depletion of glutathione (GSH) level[57]. The size of the NP alone may not be responsible for cytotoxicity, but the total particle number per unit volume may be important. Smaller particles occupy less volume and therefore larger number of particles can occupy a unit area, resulting in increased oxidative stress, ROS generation or mitochondrial perturbation[59]. Shang et al. have concluded that smaller NPs have a higher probability to be internalized by living cells and more likely cause toxic cellular responses[60].

Cellular uptake of NPs has been shown to be shape-dependent: shorter Au nanorods internalize more easily as particles with higher aspect ratio take longer time to internalize through endocytosis[28, 61]. Shape-dependence can be cell line specific. Graf et al. showed higher nanoprism uptake compared to spherical NPs by cells with flexible cell membrane compared to stiff membrane[62]. Cells with

rather stiff membrane showed no NP shape-dependent affinity[62]. Shape-related studies with fish gill epithelial cells and zebrafish embryos[63] and cell cultures[64] also indicate potential shape-specific effect of rod/wire-shaped particles.

Particle surface properties greatly influence cell-NP interactions. Surface coating may affect particle surface charge and subsequently alter particles' behaviour. Positively charged Au[65], SiO_2[66], TiO_2[67] and Ag[22] particles have been shown to associate with cells more readily compared to negatively charged particles. Surface charge also affects the cellular uptake mechanism – positively charged particles are taken up rapidly by clathrin-mediated endocytosis, but negatively charged particles show inferior rate of endocytosis[28, 68]. Ag NPs with different coating material can induce unlike toxic effects due to different ability of the coating material to complex released Ag^+ ions[46]. The fate of particles after uptake must be considered as the particles may dissolve (e.g. Ag^+ ions induce ROS directly or influence the work of ROS scavengers). The study by Jiang et al. claimed that 80% of Ag NPs taken up by the cells were dissolved after 24 h incubation and after cellular uptake silver changes overtime from Ag^0 to Ag-O- to Ag-S- form[30].

Among the listed parameters surface chemical composition/modification is claimed to be one of the most efficient means to control and modulate interactions between NPs and mammalian cells. NP's surface properties greatly depend on surrounding media: biomolecules (proteins, natural organics etc) can adsorb onto the surface and thereby functionalize the particle. A subsequent protein corona[69] formed around NPs alter the behaviour of the particle[70]. At the same time, the possibility to functionalize NPs e.g. using specific proteins enable the development of highly efficient and specific drug-delivery options. Cell-specific uptake mechanisms and pathways are essential properties when designing cancer treatment drugs which selectively kill cancer cells without affecting normal cells[71].

Due to the lack of suitable methods enabling visualization and quantification of cell-particle interactions, it is not clear whether the toxic effects of Ag NPs are caused by cell surface-bound particles resulting in local Ag dissolution or by internalized Ag NPs[32, 72]. Many microscopy techniques exist for qualitative evaluation of cell-NP interactions[73] but they often don't achieve nanoscale resolution/sensitivity (e.g. light microscopy or dark-field microscopy[74]), need specially labelled NPs (fluorescence microscopy[75]) or excessive sample preparation that may introduce possible artefacts (electron microscopy[73]) and the results can't be directly linked to quantitative toxicological results. Enhanced dark-field microscopy on the other hand is specifically designed to allow visualization of particles as small as 10 nm[76]. Flow cytometry is another promising method for studying cell-NP interactions. Cell-association of TiO_2, Ag, SiO_2 and Fe_3O_4 NPs has been characterized using flow cytometry and the detected NPs have been assumed to be intracellularized[66, 67, 77–79]. Only a few studies have attempted to quantify cell-associated NPs. For example Böhme et al. used flow cytometry together with ICP-MS to quantify the uptake of Al_2O_3 NPs by skin keratinocytes and lung epithelial cells[80]. Selective chemical etching that removes cell surface bound NPs has been utilized to distinguish between cell

surface-bound and internalized Au[65] or Ag[81] NPs, respectively. Qualitative and quantitative understanding of Ag NP-cell interactions is needed to correlate cell-NP interactions with cytotoxicity results.

3.4. Antimicrobial applications of nanoparticles

According to product inventories which list NP-containing products, majority of the listed consumer products involve antimicrobial protection[82, 83]. Antimicrobial NPs can be classified as inorganic (e.g. metal or metal oxide NPs), hybrid (e.g. surface modified metal oxide NPs) and organic (e.g. polymeric NPs) materials[84]. The listed applications include medical equipment coatings, cosmetic products, textiles, sprays etc. Depending on the (potential) NP application, the impact on target and non-target organisms needs to be evaluated as the toxic range for both types of organisms may overlap[12, 85]. The assessment of toxicity and/or safety can be complex as characteristics of NPs, the surrounding media and types of organisms all impact NP-cell interactions and toxic action. Among the biocidal NPs, Ag NPs have the most widespread use and are included in 12–24% of the listed products[82, 83].

Efficient silver-containing antibacterial systems can be developed by (i) increasing the amount of Ag used, (ii) controlling Ag NPs size, shape and coating to increase the rate of Ag^+ release or (iii) increasing Ag concentration locally by increasing affinity of NPs or Ag^+ towards bacteria[51] while remaining safe for non-target organisms. Uncertainties still exist in understanding the mechanism of Ag NP cellular interactions and toxicity. Silver compounds still need to be used with caution as increase in development of bacterial silver-resistance may occur[24, 86].

There is a growing interest in new bactericides as antibiotics resistant bacteria have become an increasing global health threat[87]. Bactericidal NMs are of great interest and amongst them, Ag is a promising alternative to antibiotics. The use of Ag NPs in combination with antibiotics has been suggested to reduce the dose of antibiotics, needed to achieve the same effect, by up to 1000-fold, therefore lowering the chances of antibiotic resistance development[88]. Ag NPs have shown to hinder the growth of bacterial biofilms, which are associated with a number of human infections[88] and therefore could be utilized in coatings of frequently-touched surfaces to reduce bacterial growth.

3.4.1. Nanomaterial-based antimicrobial coatings

Healthcare associated infections (HCAI) are a global concern and efficient antimicrobial coatings are estimated to decrease HCAI and the spread of anti-biotics resistant bacteria[89]. Strategies for antimicrobial surfaces include (Figure 2): (i) antimicrobial agent-based coatings to kill microbes due to release of active agent[90], (ii) physical surface structures or covalently anchored active substances

to kill microbes on contact[91, 92], and (iii) surface modifications (e.g. topography or altered hydrophilic/hydrophobic properties) inhibiting initial microbial adhesion[93]. Thus, antimicrobial surfaces can be classified as either antibiofouling or bactericidal[94]. Metal-based microbe inhibiting surfaces (Cu, Cu alloys or Ag) have been used for centuries[95] but as such surfaces mainly act via metal ion release[96] they are not able to degrade the remains of dead bacteria on the surface. The other downsides are the change of the material appearance due to e.g. oxidation and cost of the material[97].

Antimicrobial NPs show great promise in respective surfaces[84] as the use of NPs in surface coatings can increase surface efficiency due to large specific surface area of NPs[98]. Although not only metal-based NPs lead to antimicrobial action (e.g. chitosan NPs)[99], according to meta-analysis of scientific literature[99] and relevant consumer-product databases[82, 83] antimicrobial coatings most commonly incorporate metal (e.g. silver, titanium, copper, zinc)-based NPs.

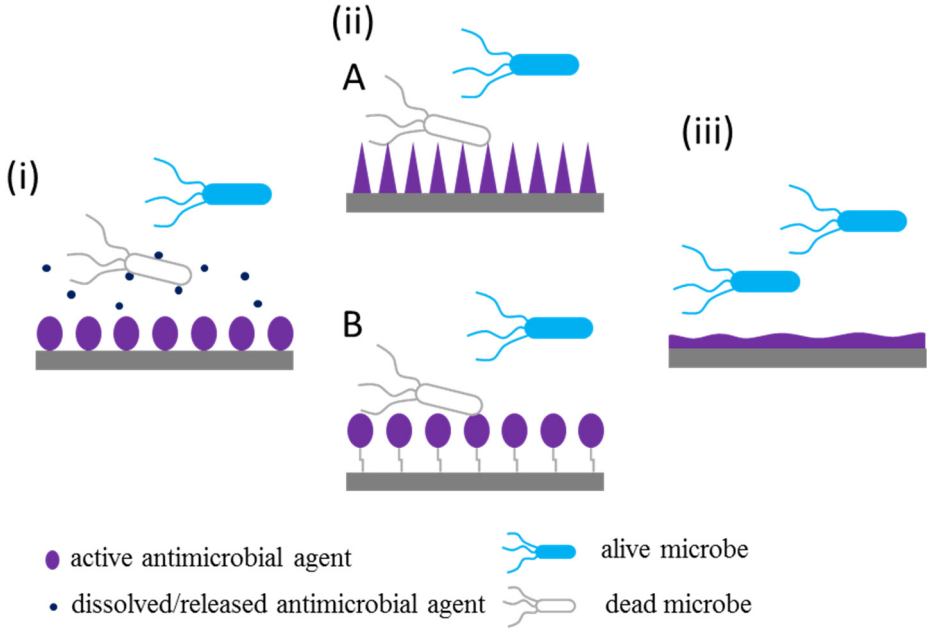

Figure 2. Scheme of different types of antimicrobial coatings. (i) antimicrobial agent release-based coating (ii) contact killing based coating (A – physical surface structure e.g. nanostructured surface, B – covalently surface-linked active agent based coating) (iii) anti-adhesion coatings. Modified from (Ahonen et al. 2017)[99].

3.4.2. Photocatalytic antimicrobial nano coatings

Photocatalyst (TiO_2[100, 101], ZnO[102]) containing antimicrobial surface is a promising approach to induce microbial killing and degradation of organic matter under specific illumination conditions in a cost-effective way. Commonly, light in the UV energy range is required to overcome photocatalyst band gap (energy required to promote electron from valence band to conduction band) and create electron-hole pairs which have the ability to produce well-known ROS: superoxide anion radicals ($\bullet O_2^-$) and/or hydroxyl radicals (•OH). The use of nanosized structures in photocatalysis-dependent antimicrobial surfaces potentially enables to prepare highly efficient surfaces as high surface area of NM ensures the presence of higher amount of surface adsorbed species that can act as electron and/or hole traps[101], therefore prolonging recombination.

TiO_2 (band gap 3.2 eV) is a well-known environmentally benign[103] photocatalyst[104], solar cell material[105], anti-fogging material and self-cleaning coating material[106, 107]. Photoactivated TiO_2 has the ability to destroy a wide range of organic contaminants including microbes. The suggested mechanism behind such behaviour is the degradation of membrane components by the ROS produced during photocatalytic processes[108–109]. TiO_2 occurs in three different crystal phases (anatase, rutile, brookite) of which anatase phase is shown to produce ROS at higher rate compared to other TiO_2 crystal phases[110]. Highly reactive hydroxyl radicals are produced during photoexcitation (generated photoholes oxidize surface absorbed H_2O)[101]. Other ROS contribute to TiO_2 photocatalytic activity, but the majority is attributed to •OH, which are shown to diffuse over short distances and therefore degrade organic compounds (including essential cellular components of microbes) that are not directly in contact with the photocatalyst[101, 111]. Thin film coatings of TiO_2 are good candidates for inhibiting the growth of potentially pathogenic bacteria[112]. A proposed alternative photocatalyst to TiO_2 is ZnO which possess similar band gap (3.37 eV) and likewise act mainly via photogenerated hydroxyl radicals but exhibit higher absorption efficiency across a large fraction of the solar spectrum[113]. ZnO NMs have reported to induce antibacterial activity through chemical (photoinduced ROS) as well as physical (mechanical damage) interactions[114] and therefore is also a potential candidate to be used in antimicrobial surface coatings.

3.4.3. Nanomaterial-based antimicrobial surfaces with combined effect of ion release and photocatalysis

A way to supress the effect of the limitation that only a small fraction of photons in solar spectrum exceeds band gap energy of the most widespread photocatalyst (TiO_2, ZnO)[115] is to deposit noble metals (e. g. Ag) on these semiconductors (Figure 3A). In this case the noble metal deposition works as an electron sink and facilitates charge separation (inhibition of recombination) and therefore increases efficiency of photocatalysis (Figure 3B)[116]. Other possibilities include band gap

narrowing by incorporating metal atoms into crystal lattice[117] or visible light plasmonic absorption on metal deposits with following energy transfer to semiconductor. The combination of TiO_2 or ZnO with Ag deposits is a promising approach to create antimicrobial materials[118]. The increased antimicrobial effect of nano-composite semiconductor materials (e.g. ZnO+Ag) rises from improved photocatalytic activity and/or the release of toxic ions (Zn^{2+}, Ag^{+}). Ag doped ZnO NPs have reported to induce enhanced antimicrobial activity compared to pure ZnO[119]. Heterostructured Ag-ZnO nanorod arrays possess higher antimicrobial efficiency compared to bare ZnO nanorod arrays and neither arrays showed cytotoxicity towards mouse fibroblast cell line[120], which motivate the use of Ag-ZnO combination in development of antimicrobial surfaces with low potential toxicity towards human.

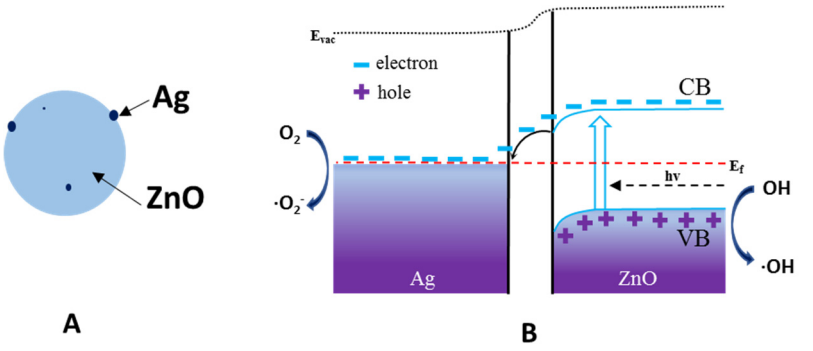

Figure 3. Schematic illustration of Ag deposits on ZnO (A) and the proposed charge separation process and photocatalytic ROS generation of ZnO/Ag structures under UV-light (B). As the energy level of ZnO conduction band (CB) is higher than Fermi energy level (E_f), photoinduced electrons are transferred from ZnO to Ag. Subsequently, electrons in the Ag sinks react with chemisorbed O_2 (forming superoxide: $\cdot O_2^-$) and holes react with surface hydroxyl OH (forming hydroxyl radicals: ·OH). VB – valence band, E_{vac} – vacuum level. Modified from (Lu et al. 2008)[116].

3.4.4. Preparation and efficiency testing of nanomaterial-based antimicrobial surfaces

To prepare antimicrobial surfaces from NPs, the particles may be fabricated directly onto various supports[121] or previously synthesized NPs can be deposited on a surface using e.g. spin-coating, drop-casting, spray-coating or electrophoretic deposition[122]. NP production can be very broadly classified into a top-down (material is decreased from large to nanoscale) and a bottom-up (NP production starts from the atomic level) approach. There are various methods for the synthesis of NPs but in the case of TiO_2 and ZnO, solution-based approach (e.g. hydrothermal synthesis) has been claimed to be the simplest and the least energy consuming[113]. Metal NPs are mainly synthesized using a chemical, physical or even biological method[123]. Chemical reduction is the most often

applied method for the preparation of stable metal NP suspensions[123]. In the case of preparing Ag NPs, a soluble metal salt (e.g. $AgNO_3$) is often used as a source for Ag^+ ions. The reduction of ions can be carried out using a reducing agent (chemical reduction)[124] or irradiation (photoreduction)[125] and the resulting Ag^0 atoms form NPs.

In the case of photocatalytic materials, the photodegradation efficiency of surfaces is evaluated. Similarly to suspensions of photocatalytic particles which are mixed with solutions of model organic dye[115] the NP covered surfaces are often suspended in a model dye solution[126]. After appropriate irradiation times the absorbance of model dye solution is measured to evaluate the photodegradation efficiency of the suspended particles or surfaces[115, 126].

There is no widely accepted methodology available to precisely and reproducibly evaluate the antimicrobial efficiency of NM-based antimicrobial surfaces[127]. The antimicrobial efficiency of conventional surfaces is evaluated using zone of inhibition, immersive inoculation, direct inoculation or surface growth methods[128]. The three major international standards for the assessment of antimicrobial activity of surfaces are JIS Z2801:2010 (Antibacterial products – Test for antibacterial activity and efficacy), ISO 22196:2010 (Measurement of antibacterial activity on plastics and other non-porous surfaces) and US EPA (Protocol for the evaluation of bactericidal activity of hard, non-porous copper containing surface products)[97]. The standards use *Staphylococcus aureus*, *Escherichia coli* or *Pseudomonas aeruginosa* suspensions to inoculate the test surface. After 24 h incubation the inoculum is washed off and colony counting on agar plates is used to assess the bactericidal efficiency of the tested surface. The need to use UV-light to activate photocatalyst-containing surfaces complicates the testing procedure but there is a standard (ISO 27447:2009) for testing antimicrobial properties of semiconducting photocatalytic materials[129]. The present thesis addressed the need for more suitable testing methods to allow higher throughput screening of antimicrobial properties of NM-based surfaces by modifying and improving the available testing standards.

4. MATERIALS AND METHODS

4.1. Materials

Reagent grade chemicals and water purified with MilliQ equipment were used throughout the experiments. Ag NPs used in the studies were bought: Paper I – Ag nanowires in powder form from Seashell Technology (USA), Paper I and II – citrate stabilized Ag nanosphere aqueous suspensions from MKNano (Canada); Paper III – citrate, bPEI and PEG stabilized Ag nanosphere aqueous suspensions of different sizes from nanoComposix (USA). Self-built fluorescent Hg lamp consisting of fluorescent light bulbs (15 W iSOLde Cleo, λ_{max} 355 nm) was used in Paper IV (light intensity at sample height in 315–400 nm spectral region was 22 W/m^2) and Paper V (light intensity at sample height in 315–400 nm spectral region was 2.7–3.2 W/m^2) for UVA-light exposures.

4.2. Nanomaterial preparation methods

Ag nanowires were suspended and sonicated (40 W probe sonication for 1.5–2.5 min) before experiments. Ag nanosphere stock suspensions were diluted to relevant test concentrations using water (bacterial assay – Paper I and II; particle characterization analysis – Paper I, II, III; dissolution study – Paper I and II) or cell culture media (mammalian cell assays – Paper II and III; dissolution study – Paper III) depending on the experimental setup and requirements. The exact Ag concentrations in suspensions were determined by ICP-MS or AAS.

Metal oxide NPs were prepared by hydrothermal synthesis. TiO_2 particles were synthesized using PTSA, $Ti(OBu)_4$ and acac as starting materials. The reaction was carried out overnight at reflux conditions and reaction product was subsequently washed with methanol and dispersed in ethanol (Paper IV). ZnO particles were synthesized using Zn-acetate and KOH in methanol. The reaction was carried out at reflux conditions for 72 h. The reaction product was washed with methanol and redispersed in butanol. Acac was added as a stabilizing ligand. ZnO/Ag composite particles were synthesized by photodeposition of Ag from Ag^+-containing complex (silver 2-ethylhexanoate) onto ZnO particles using UVA-diode irradiation (120 W/m^2). The product was washed with butanol (Paper V).

Thin films and NP covered surfaces were prepared by spin-coating aliquots of colloidal solution on ethanol or acetone washed silicon or glass substrates at ambient atmospheric conditions. TiO_2 thin films were aged at ambient conditions to allow evaporation of remaining solvent, subsequently annealed at 400 °C and washed in deionised water in ultrasonic bath to remove organic residue. ZnO and ZnO/Ag composite NP covered surfaces were heated at 200 °C for removal of organic residue.

4.3. Characterization of particles and surfaces

NPs and NP covered surfaces were extensively characterized to interpret and report the results as accurately as possible. The primary size of NPs was measured using SEM (Paper I) or TEM (Paper II, III, V). Hydrodynamic size and particle surface charge (zeta-potential) were measured using dynamic light scattering (DLS) and electrophoretic light scattering, respectively (Paper I, II, III and IV). Elemental analysis of NPs and NP suspensions was done by SEM-EDX mapping (Paper I and II), STEM-EDX mapping (Paper V), TXRF or AAS (Paper I, II, III, V). Elemental analysis of NP covered surfaces was carried out by acid digestion of surface coating followed by TXRF or AAS (Paper V). UV-Vis spectroscopy was used to detect Ag characteristic surface plasmon resonance peak (Paper I, II and V) and evaluate indirect optical band gap of TiO_2 (Paper IV). Surfaces containing NPs were characterized using Raman spectroscopy (Paper IV) or XRD (Paper V) to confirm crystalline structures and SEM (Paper IV, V) to visualize surface morphology.

As Ag and ZnO particles are known to dissolve and Ag^+ and Zn^{2+} ions have been shown to exhibit antimicrobial effect, ion release from NPs or NP covered surfaces was analysed. Ag NPs were incubated in conditions (exposure media and time) used in bioassays after which they were ultracentrifuged to separate particulate and ionic form. The resulting supernatant was analysed by AAS (Paper I and II) or ICP-MS (Paper III). Zn and Ag release from ZnO and ZnO/Ag composite NP covered surfaces was measured by exposing surfaces to conditions analogous to antimicrobial test after which Zn and Ag content in the washoff was analysed by TXRF or AAS. The possibility of release of NPs during antimicrobial testing of NP covered surfaces was checked by ultracentrifugation and subsequent chemical analysis of washoffs from 60 min incubated surfaces (Paper V).

4.4. Antimicrobial activity, bioavailability, ROS production and toxicity of Ag nanoparticles (Paper I, II, III)

Model gram-negative bacterium *E. coli* (Paper I, II) was used in antimicrobial tests. Murine fibroblast cell line Balb/3T3 (Paper II) and Jurkat human T-lymphocyte cell line (Paper III) were used in cell culture studies.

Generally, in antimicrobial tests bacterial suspensions were prepared in appropriate concentrations and exposed to relevant concentrations of Ag NPs on the microplate. Depending on the organism and the assay, either inhibition of bioluminescence and/or inhibition of bacterial growth was used as an endpoint to determine half-effective concentration value (EC_{50}). Usually, tests were repeated on separate days to account for inherent variability of bioassays. $AgNO_3$ was used as an ionic control, samples not exposed to NPs as the negative controls. In Paper I and II bacterial assays were conducted in MilliQ water to avoid the potential

impact of Ag speciation on the test results. Bioavailability of Ag^+ ions was evaluated by monitoring bioluminescence induction of Ag^+-induced *E. coli*. Induction value of 2 was considered as induction threshold. EC_{50} values were normalized according to Ag NP dissolution and/or bioavailability. H_2DCFDA indicator was used to evaluate the Ag NP abiotic ROS production potential. Increase in dye fluorescence was measured (Paper II).

Cell culture assays for toxicity evaluation were performed on microplates in cell culture media. Cells were exposed to Ag NPs at 37 °C and 5% CO_2. After 24 h incubation cell viability was assessed using Neutral Red (Paper II) or resazurin assay (Paper III). $AgNO_3$ was used as an ionic control, samples not exposed to NPs as negative controls.

4.5. Analysis of cell-particle interactions (Paper III)

Cell-particle interactions were studied using imaging flow cytometry and enhanced dark-field microscopy. For imaging flow cytometry analysis, the cells were washed and resuspended in PBS after exposure. For live-dead analysis the cells were stained with fluorescein diacetate and propidium iodide. Information in bright field, dark field, and fluorescence was collected in parallel. Separate compensation samples were used to take into account background signals. Same exposed suspension was used for cell counting and the remaining suspension was acid digested and analysed with ICP-MS for Ag content. To distinguish internalized Ag from cell surface-bound Ag, selective chemical etching was used. Exposure to the mixture of $K_3Fe(CN)_6$ and $Na_2S_2O_3 \cdot 5H_2O$ in PBS was used to oxidize and complex cell surface-associated Ag. Both etched and not etched samples were analysed by flow cytometry and ICP-MS as described above. Enhanced dark-field microscopy was used for high resolution visualization. After exposure cells were washed and resuspended in PBS and fixed with formaldehyde. Drop of suspension was placed on a glass slide, mounting medium was added, the suspension was covered with cover glass and imaged.

4.6. Analysis of bacterial cell morphological changes and degradation of bacterial membrane associated fatty acids (Paper IV)

For analysis of bacterial cell morphological changes, similar exposure conditions as for viability evaluation were used for a constantly bioluminescent *E. coli* strain. In addition, 40 and 60 min exposure times were applied. After exposure the samples were fixed using 2.5% glutaraldehyde and dehydrated with ethanol. The samples were left to dry for 3 days after which they were imaged using SEM.

Uniform layer of fatty acid (stearic, oleic and linoleic acid) was spin-coated onto nano-TiO_2 thin film substrate for photoactivated degradation studies. UVA

exposure was carried out in a climate chamber (25 °C, 70% rh) for 0, 1, 3, 5 and 10 min. Changes in fatty acid chemical structure were evaluated by measuring carbon 1s XPS spectra (comprising sp^2 carbon, sp^3 carbon and carboxylic group) after each exposure using a surface station in the Institute of Physics, University of Tartu.

4.7. Antimicrobial activity of nanoparticle covered surfaces (Paper IV, V)

Gram-negative bacterium *E. coli* (IV and V), gram-positive bacterium *S. aureus* (Paper V) and fungi *C. albicans* (Paper V) were used as model organisms to evaluate the antimicrobial properties of NP covered surfaces.

Photocatalytic metal oxide NP covered surfaces were tested for their antimicrobial effect under UVA light. Two different protocols were used. In Paper IV, aliquots of bacterial suspension of a constantly bioluminescent strain of *E. coli* were dropped onto the surfaces and exposed to UVA (22 W/m^2). After exposure (0, 5, 10, 15 and 20 min) in a climate chamber (25 °C, 90% rh) bacteria were washed off from the surfaces, serially diluted and aliquots of each dilution were spread onto LB agar plates. After overnight incubation at 37 °C colonies were counted. In Paper V, test protocol modified from ISO 27447:2009 was used for higher throughput. Aliquots of microbial suspensions were applied to the test surface and covered with polyethylene film. Exposure to UVA (2.7–3.2 W/m^2) was carried out in humid environment. After exposure microbes were washed off from the surfaces with toxicity neutralizing agent. The washoff was serially diluted and each dilution was drop-plated onto nutrient agar plates. After 24–48 h incubation at 30 °C colonies were counted. In Paper V antimicrobial activity of Zn^{2+} ions (from soluble $ZnSO_4$) was evaluated by exposing microbial suspension containing relevant concentration of Zn^{2+} ions on an untreated glass substrate to UVA light. Exposure on non-coated substrates and samples kept in the dark were used as controls in both studies.

4.8. Photocatalytic properties of nanoparticles and nanoparticle covered surfaces (Paper V)

Photocatalytic properties of NP suspensions were evaluated. Photodegradation of added model dye (brilliant blue FCF) was monitored after exposure using UV-Vis spectroscopy.

4.9. Reusability of nanoparticle containing surfaces (Paper V)

10 cycles of use and cleaning were applied to ZnO/Ag composite NP covered surfaces. Antibacterial efficiency was evaluated after each cycle. Photocatalytic activity measurements, elemental analysis and SEM imaging were done on unused surfaces and surfaces after 3 and 10 use cycles.

4.10. Statistical analysis

MS Excel was used to calculate standard deviations and perform t-test. GraphPad Prism or Excel Macro Regtox (MSExcel macro REGTOX EV7.0.5.xls, available online at: https://www.normalesup.org/~vindimian/en_index.html) was used for EC_{50} calculations. One-way ANOVA followed by Tukey's HSD using R was performed to detect statistically relevant differences in viable counts in Paper V.

5. RESULTS AND DISCUSSION

5.1. The effect of Ag nanoparticle shape, size and surface charge on antimicrobial activity and toxicity (Paper I, II, III)

As the effects of chemicals and materials (including NPs) are directed towards certain target organisms, the impact on so-called non-target organisms must be as low as possible. In the case of antimicrobial substances, humans are considered non-target organisms. Therefore, alongside antimicrobial studies towards bacteria cytotoxicity towards mammalian cells was evaluated.

To study the potential shape- and size-dependent effects of Ag NPs towards bacterial and mammalian cells, a library of particles was tested (Table 1). Ag nanospheres (Ag NSs, 83 nm) were tested alongside Ag nanowires (Ag NWs, 100 nm × 6100 nm) to study shape-dependent antibacterial activity (Paper I) (Figure 4). The diameters of the tested nanospheres and -wires were chosen in the same size range to enable relevant comparison. Different-sized citrate-coated spherical particles (10, 20, 40, 60 and 80 nm) (Figure 5 A) were tested towards model bacteria *E. coli* and mammalian fibroblasts to evaluate size-dependent antimicrobial activity and toxicity of Ag particles (Paper II). Particle sizes discussed hereafter are mean particle diameters, size distributions are shown in Table 1. In addition to primary size the hydrodynamic size of the tested particles in the used test media was measured to adequately interpret toxicity results. Bacterial assays in Paper I and II were conducted in MilliQ water to exclude Ag speciation driven alterations and the hydrodynamic size in MilliQ water was close to NP primary size. Hydrodynamic diameters in cell culture medium were bigger compared to MilliQ water. The increase is due to organic components found in the media which form a surface coating on the particles[70] (Table 1).

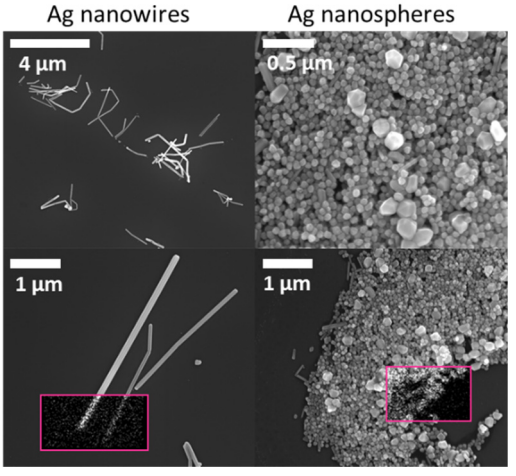

Figure 4: Scanning electron micrographs and EDX mapping (insets showing Ag L_α signal) of Ag nanowires and Ag nanospheres.

EC_{50} values calculated from bioluminescence inhibition (Table 2) showed statistically significant difference between Ag NSs and Ag NWs which indicated possible shape-dependent antibacterial activity towards *E. coli*. Size-dependent antibacterial activity and cytotoxicity was observed when 10 nm to 80 nm Ag nanospheres were tested towards bacterial and mammalian cells. The results showed that both increased (i.e. EC_{50} and IC_{50} values decreased) with decreasing particle size (Table 2).

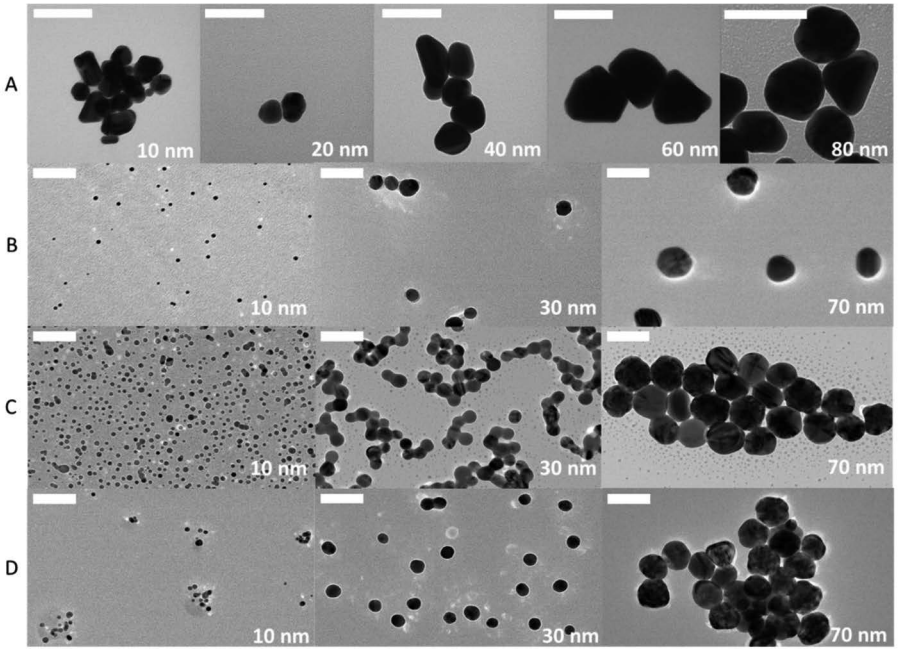

Figure 5. Transmission electron microscopy images of Ag nanoparticles (NPs). A – 10, 20, 40, 60 and 80 nm Ag NPs (Paper II). B – 10, 30 and 70 nm bPEI-coated Ag NPs (Paper III). C – 10, 30 and 70 nm PEG-coated Ag NPs (Paper III). D – 10, 30 and 70 nm citrate-coated Ag NPs (Paper III). Scale bars represent 100 nm.

The influence of surface charge (positive, negative and near neutral) on cytotoxicity was studied using human T-lymphocyte cell line (Paper III). Homogenous and well dispersed Ag NPs with different surface coatings (bPEI, citrate, PEG) were tested (Figure 5 B, C, D). Surface charge measurements confirmed different surface charges: bPEI-coated particles had positive surface charge (33 to 42 mV), citrate covered particles negative (–39 to –44 mV) and PEG covered particles lower negative charge (–21 to –22 mV) (Table 1). The low negative charge is hereafter referred to as near neutral surface coating as the surface charge value of PEG covered particles is the closest to 0 compared to other two surface charges. PEG-coated (near neutral) and citrate-coated (negative) particles were less toxic than bPEI-coated (positive) particles (Table 2). High toxicity of cationic Ag particles could be due to (i) strong binding to cell surface followed by release of Ag^+ ions, (ii) direct damage to cell membrane, or (iii) elevated cellular uptake.

Table 1. Physico-chemical properties of Ag NPs with different shape, size and surface charge (Paper I, II, III)

Particle	Primary size, nm	Hydrodynamic size (pdi) in MilliQ water, nm	Hydrodynamic size (pdi) in cell culture medium, nm	Surface coating	Surface charge in water, mV	Surface charge in cell culture medium, mV	Paper
Ag NWs	100±40 x 6100±2700	not relevant	–	n.a.	–46	–	I
Ag NSs	83±37	98±1.8 (0.25)	–	citrate	–36	–	I
$citrate_{MK}$-Ag 10 nm	11.6±5.2	6 (0.48)	68.6 (0.29)	citrate	–25	–9.59	II
$citrate_{MK}$-Ag 20 nm	17.8±8	11 (0.43)	76 (0.31)	citrate	–25	–10	II
$citrate_{MK}$-Ag 40 nm	47.7±8	16 (0.28)	107 (0.26)	citrate	–24	–4.84	II
$citrate_{MK}$-Ag 60 nm	56.5±9.6	58 (0.25)	162 (0.14)	citrate	–15	–8.29	II
$citrate_{MK}$-Ag 80 nm	94.8±54	68 (0.3)	153 (0.23)	citrate	–16	–9.2	II
bPEI-Ag 10 nm	9.2±1.1	15.7±6.9	89.9±46.8	bPEI	+33.4±0.4	–	III
bPEI-Ag 30 nm	29.3±4	58.0±15.3	237±147	bPEI	+36.5±1.2	–	III
bPEI-Ag 70 nm	79.4±4.3	87.9±27.3	343±140	bPEI	+42.1±2.6	–	III
PEG-Ag 10 nm	9.7±1.4	18.1±9.0	73.0±31.0	PEG	–20.8±2.1	–	III
PEG-Ag 30 nm	29.1±2.6	39.7±10.8	57.3±28.9	PEG	–22.7±1.1	–	III
PEG-Ag 70 nm	70.5±7.7	78.8±19	113±69.8	PEG	–22.2±1.1	–	III
citrate-Ag 10 nm	9.8±1.5	9.6±3.4	42.2±31.5	citrate	–39.6±0.71	–	III
citrate-Ag 30 nm	28.7±2.7	40.2±19.0	50.7±37.0	citrate	–39.7±0.6	–	III
citrate-Ag 70 nm	71.5±5.8	79.2±24.1	87.3±28.9	citrate	–44.1±0.4	–	III

pdi – polydispersity index ; NWs – nanowires; n.a. – not available; NSs – nanospheres; bPEI – branched polyethylenimine; PEG – polyethylene glycol

Table 2. Nominal, dissolution corrected and bioavailability corrected EC_{50} and IC_{50} values for Ag NPs (Paper I, II, III)

Particle/Chemical	Antibacterial activity: EC_{50}, µg/mL	EC_{50} corrected to Ag dissolution [1]	EC_{50} corrected to bioavailability [2]	Cytotoxicity: IC_{50}, µg/mL	IC_{50} corrected to Ag dissolution [1]	Paper
Ag NWs	0.42±0.06 [a, *]	0.011±0.0014	0.011±0.005	–	–	I
Ag NSs	0.68±0.01 [a, *, **]	0.015±0.0002	0.0099±0.004	–	–	I
$AgNO_3$	0.0082 [a]	0.0082	0.0083	–	–	I
$citrate_{MK}$-Ag 10 nm	0.27±0.2 [b, *]	0.004±0.0026 [*]	0.012±0.00011	16.9±1.9 [c, *]	1.18±0.14	II
$citrate_{MK}$-Ag 20 nm	0.51±0.24 [b, *]	0.006±0.003	0.016±0.00009	22.0±1.3 [c, *]	1.76±0.11	II
$citrate_{MK}$-Ag 40 nm	1.51±1.12 [b, *]	0.012±0.0091	0.016±0.0001	28.7±1.6 [c, *]	1.48±0.09	II
$citrate_{MK}$-Ag 60 nm	2.56±1.6 [b, *]	0.017±0.011	0.020±0.00009	30.9±2.1 [c, *]	1.65±0.12	II
$citrate_{MK}$-Ag 80 nm	2.96±1.83 [b, *]	0.019±0.012	0.020±0.00008	34.9±2.3 [c, *]	2.62±0.17	II
$AgNO_3$	0.010±0.004 [b]	0.010±0.004	0.010±0.004	1.70±0.57 [c]	1.70±0.58	II
bPEI-Ag 10 nm	–	–	–	3.4±0.4 [d]	0.83±0.10	III
bPEI-Ag 30 nm	–	–	–	6.6±0.6 [d]	0.89±0.08	III
bPEI-Ag 70 nm	–	–	–	14.0±4.2 [d]	0.78±0.24	III
PEG-Ag 10 nm	–	–	–	11.2±5.2 [d, ***]	3.46±1.61	III
PEG-Ag 30 nm	–	–	–	17.7±4.7 [d, ***]	3.33±0.88	III
PEG-Ag 70 nm	–	–	–	44.2±18.2 [d, ***]	5.92±2.44	III
citrate-Ag 10 nm	–	–	–	8.9±4.1 [d, ***]	2.67±1.23	III
citrate-Ag 30 nm	–	–	–	31.4±9.0 [d, ***]	4.18±1.20	III
citrate-Ag 70 nm	–	–	–	42.6±18.0 [d, ***]	4.09±1.73	III
$AgNO_3$	–	–	–	0.58±0.11 [d]	0.58±0.11	III

EC_{50} – half-effective concentration, bacteria; IC_{50} – half-inhibitory concentration, mammalian cells; NWs – nanowires; NSs – nanospheres; bPEI – branched polyethylenimine; PEG – polyethylene glycol; [a] – *E. coli* MC1061(pSLlux), bioluminescence inhibition assay; [b] – *E. coli* K12 (BW30270), viability assay; [c] – murine fibroblast cell line BALB/3T3, Neutral Red assay; [d] – human T-lymphocyte cell line Jurkat, resazurin assay; [1] – after abiotic incubation particle suspension was ultracentrifuged and supernatant analysed for Ag using GF-AAS or ICP-MS; [2] – bioavailability of silver ions from Ag NPs determined using *E. coli* MC1061(pSLcueR/pDNPcopAlux); [*] – significantly different ($p<0.05$) from ionic control ($AgNO_3$); [**] – significantly different ($p<0.05$) from ionic control ($AgNO_3$) and Ag nanowires; [***] – significantly different ($p=0.05$) from same-sized bPEI-coated Ag NPs

5.2. The effect of Ag nanoparticle dissolution and nanoparticle-cell interactions on antimicrobial activity and toxicity

To further clarify the mechanisms behind Ag NP biological effects, the tendencies observed earlier – increasing antibacterial activity and cytotoxicity with decreasing particle size and increased cytotoxicity for positively charged particles, were further combined with results from Ag NPs dissolution. Ag NPs are known to dissolve in some degree and antimicrobial activity of Ag^+ ions is well recognized[130–132]. Therefore, every study that involves Ag particles should take into consideration particle dissolution and subsequent ion-based effects. As mammalian cells can internalize particles, Ag NP-cell interactions including particle intracellularization were also studied to understand the exact processes behind the observed cytotoxicity results.

5.2.1. The effect of Ag nanoparticle dissolution on antimicrobial activity and toxicity (Paper I, II, III)

Nominal EC_{50} values indicated shape-dependent antibacterial activity when Ag NWs and Ag NSs of similar diameter were tested (Table 2). However, when the results were normalized to the concentration of dissolved Ag (2.2–2.4% of the particles dissolved to ionic form) EC_{50} values of both Ag NPs were not statistically significantly different from EC_{50} value of the ionic control ($AgNO_3$) (Table 2). That suggests that the effects were driven by dissolved Ag^+ ions. Same conclusion was drawn when initial EC_{50} values were normalized to bioavailable Ag (Table 2) using Ag^+-induced *E. coli*[133]. Antibacterial activities of Ag NWs suspension and its ultracentrifuged particle-free supernatant were equal further proving ionic toxicity mechanism (Paper I Figure 4 a). Viability assay showed remarkable decrease in bacterial cell count at 5–9-fold higher concentrations (Paper I Figure 4 b). The inhibition of bacterial bioluminescence can therefore be considered an adequate indicator for toxicity that reflects changes in bacterial energy metabolism[134] and correlates significantly with cellular viability[135]. Although no shape-dependent effects were seen with ~80 nm diameter particles (nanospheres vs nanowires), shape-dependence may still occur with smaller sized particles. Indeed, shape-dependent antibacterial effect for Ag particles has been reported[49, 50, 52] but the dissolution of the particles and influence of Ag^+ ions wasn't evaluated in those studies. Therefore, it can't be ruled out that the observed effects could have been explained by particle dissolution as particle shape affects particle dissolution[62].

The influence of particle dissolution on the observed size-dependent antibacterial efficacy and cytotoxicity results for 10 nm to 80 nm diameter Ag particles ($citrate_{MK}$-Ag) was assessed. Increased dissolution with decreasing particle[136] size was observed which could be explained by increased specific

surface area of smaller particles. Nominal EC_{50} values were corrected to dissolution (Table 2) and it was concluded that dissolution fully explained the antimicrobial activity of 20 nm to 80 nm diameter particles towards bacterial cells and toxicity of all the particles towards mammalian cells.

It seemed that 10 nm particles had additional non-dissolution driven antibacterial properties as the efficacy was higher than could be predicted from EC_{50} value of ionic control ($AgNO_3$) (Table 2). At the same time similarities in the slopes of dose-response curves for $AgNO_3$ and Ag NPs indicate that all the tested Ag compounds have a common mechanism of action (dissolved silver) (Paper II Figure 4). The hypothesis then was that 10 nm particles may induce increased bioavailability of Ag and/or induce ROS. The formation of abiotic ROS was studied by monitoring fluorescence change of ROS-sensitive dye (H_2DCFDA) and in our case ROS was not detected at toxicologically relevant concentrations. In close contact with NPs, cells may release and import higher concentrations of metals than are dissolved in abiotic conditions[21] and thus, a more relevant measure for NP-released Ag^+ ions than centrifugation and bulk assessment of Ag should be used. For that, we measured bioavailability of Ag^+ ions using Ag^+-induced *E. coli*[133]. Concentration at which bioluminescence induction of sensor bacteria occurred decreased with decreasing particle size which correlates with increased dissolution of smaller particles. Bioavailability corrected EC_{50} values indicated that intracellular bioavailable Ag explained the antibacterial efficacy for all the tested particles, including 10 nm particles (Table 2). Thus, we conclude that the major antibacterial effect of Ag NPs derives from their enhanced local dissolution leading to increased bioavailability of Ag. Mechanism through which ions become more bioavailable than abiotic dissolution suggests is claimed to be the increased adherence of Ag particles onto bacterial cell[22]. It is known that direct contact is essential for increased bioavailability[21]. Therefore, the reason for the increase might be greater particle-cell contact and subsequent increased particle dissolution in close vicinity of the bacterial cell.

Although dissolution and release of Ag^+ ions explained the effect of variously sized Ag NPs toward mammalian cells, Ag^+ ions did not explain differences between differently charged particles. Cytotoxicity results showed increased toxic effect for positively charged particles but no obvious differences in dissolution of differently coated particles was observed (Paper III Table 1). It has been shown that cationic NPs have elevated cellular binding compared to anionic NPs[22, 60] but the difference is rarely quantitatively assessed. Therefore NP-cell interactions with differently coated Ag particles were further studied with combined complementary analytical methods to qualitatively and quantitatively evaluate the difference.

5.2.2. Analysis of Ag nanoparticle-cell interactions affecting particle cytotoxicity (Paper III)

A set of analysis methods (imaging flow cytometry, ICP-MS, dark field microscopy) was used to study NP-cell interactions. Flow cytometry relies on increased light scattering ability of cells upon their association with NPs. Flow cytometry side scatter (SSC) signal has been shown to describe cell-NP interactions[77, 78]. Imaging flow cytometry enables high-throughput semi-quantitative analysis of the level of cellular interaction with NPs and cell viability when bright field, dark field and fluorescence images are collected simultaneously. No significant increase in flow cytometry SSC signal or obvious binding in dark field microscopy was seen with most PEG- (near-neutral surface charge) and citrate- (negative surface charge) coated Ag particles. Only cells exposed to the largest tested concentration (25.0 μg/mL) of 70 nm PEG- and citrate-coated particles showed slight increase in SSC signal.

However, notable increase in SSC signal was revealed after 24 h exposure to bPEI-coated (positive surface charge) particles at a concentration as low as 0.1 μg/mL (Figure 6, Table 3). bPEI coated particles were also seen to interact tightly with cells under enhanced dark field microscope which allows visualization at higher magnification (Paper III Figure 3). In both, imaging flow cytometry and dark field microscopy, in the case of larger particles the binding of particles to cells was more obvious. Cell counting and ICP-MS analysis was used to obtain quantitative results for cell-bound Ag. The analysis revealed that although larger particles were more visible in flow cytometry and dark field microscopy, the amount of Ag bound to each cell was similar for all bPEI-coated particles. ICP-MS analysis further clarified that compared to bPEI-coated particles, the cellular binding of citrate-coated and PEG-coated particles was 4-fold and 25-fold lower, respectively (Table 3).

Cellular localization of Ag particles was analysed using selective chemical etching[81] which allowed to separate cell surface associated and intracellular Ag. The removal of cell surface associated particles was observable from changes in the flow cytometry SSC signal (Figure 7). It was seen that at IC_{50} concentration the total amount of Ag NPs bound to cells was higher for bPEI-coated particles, but intracellular concentration of Ag was remarkably similar (Table 3). Therefore, we suggest that the cytotoxicity of different Ag NPs is mostly influenced by their internalization capability and is not directly influenced by cell surface associated Ag NPs. Dissolution of internalized Ag particles has been indicated[30, 137] and therefore we indirectly evaluated the dissolution of internalized Ag NPs by comparing intracellular concentrations of Ag at IC_{50} values of Ag NPs and $AgNO_3$. The analysis revealed 4.5–9-fold higher intracellular Ag concentrations in the case of Ag NP-exposed cells suggesting that significant fraction of Ag NPs was present in nanoparticulate form.

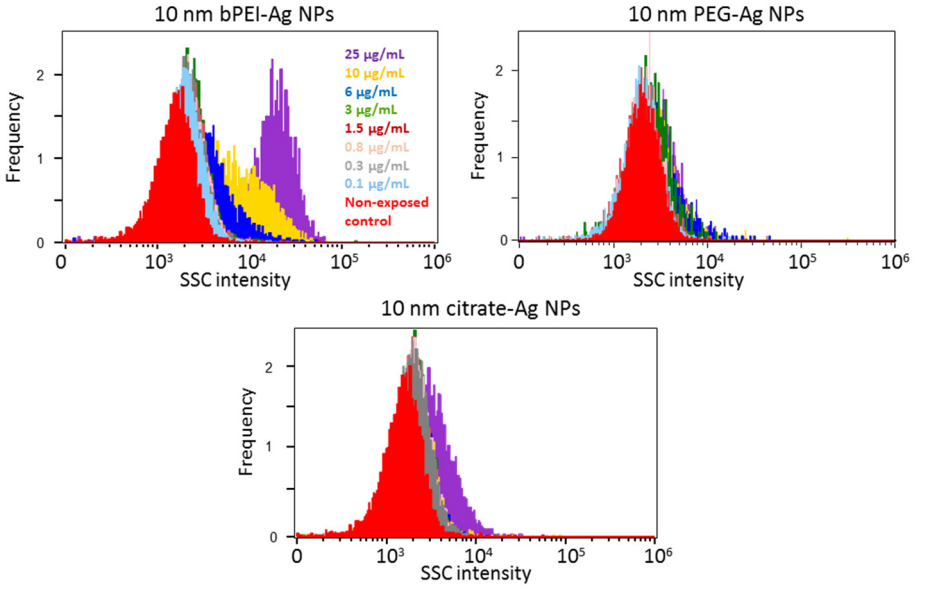

Figure 6. Association of 10 nm bPEI- (positive surface charge), PEG- (near neutral surface charge) and citrate- (negative surface charge) coated Ag nanoparticles (NPs) with human T-lymphocyte cells according to imaging flow cytometry histograms. SSC — side scatter indicating cell-associated Ag NPs.

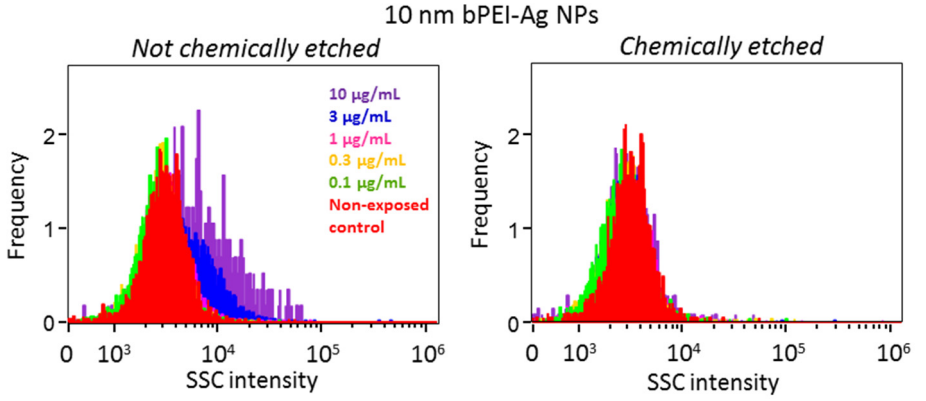

Figure 7. The effect of removal of cell surface associated 10 nm bPEI-coated Ag nanoparticles (NPs) with chemical etching according to flow cytometry histograms. SSC – side scatter indicating cell-associated Ag NPs.

It has been claimed in previous studies[77, 78] that flow cytometry analysis provides mainly information about intracellular NPs. Our study revealed that after chemical etching of surface-bound particles SSC signal disappeared. Thus, we suggest that SSC signal mainly originates from surface-associated particles. ICP-MS analysis showed that although etching removed significant fraction of Ag (as average 85%, 67% and 62–79% of bPEI-, citrate- and PEG-coated particles, respectively), there was still clear difference between intracellular concentrations of Ag NPs with different coatings at the same exposure concentrations (Paper III Figure 5). Decreased cellular uptake with increased particle size was also seen and the result is consistent with previous studies[58, 60]. As Ag NPs are suggested to be internalized through clathrin or caveolin-mediated endocytosis[29] high-affinity binding of cationic particles to cellular membrane explains the increased endocytosis activity.

On the basis of our study we recommend not to use positively charged Ag particles in antimicrobial applications as more intracellularization occurs and particles tend to be more toxic to mammalian cells than negatively and near-neutrally charged particles. Our results indicate that mammalian cells are less susceptible to Ag toxicity than bacteria (IC_{50} values ~10 times higher; Table 1) whilst it has been shown that the toxic range of Ag NPs to bacteria and mammalian cells may overlap[12, 15]. Thus, the toxicity of particles towards non-target organisms still needs to be considered when following a safe-by-design principle in product development.

Table 3. Cell-associated (sum of cell surface bound and intracellular) and intracellular Ag in Ag NP and $AgNO_3$ exposed human T-lymphocyte Jurkat cells at different 24 h exposure conditions (Paper III)

Particle code	Exposure concentration, ng/mL					IC_{50}, µg/mL	Cell-associated Ag [a] (fg Ag/cell) at IC_{50}	Intracellular Ag [b] (fg Ag/cell) at IC_{50}
	100	300	1000	3000	10,000			
	Cell-associated Ag [a] (fg Ag/cell)							
bPEI-Ag 10 nm	12.8±13.0	26.6±13.9	68.0±6.1	254±75.3 *	n.a.	3.4±0.4	462±47.6	47.3±4.8
bPEI-Ag 30 nm	8.8±3.2	26.5±17.6	46.8±35.9 *	217±127 *	571±248 *	6.6±0.6	386±33.4	62.2±4.5
bPEI-Ag 70 nm	7.9±2.1	23.5±15.5 *	82.5±44.5 *	321±145 *	664±348 *	14.0±4.2	954±286	56.9±11.1
PEG-Ag 10 nm	0.5±0.1	0.5±0.4	4.9±2.0	21.0±10.5	60.0±21.6	11.2±5.2	93.9±24.9	39.8±23.7
PEG-Ag 30 nm	0.3±0.1	0.6±0.3	4.2±1.9	22.0±18.6	63.9±35.4	17.7±4.7	124±30.4	38.4±10.4
PEG-Ag 70 nm	0.2±0.1	0.4±0.3	3.7±1.6	15.0±11.5	40.5±22.4	44.2±18.2	181±74.6	37.4±10.3
citrate-Ag 10 nm	6.2±3.8	10.4±7.9	31.4±13.9	61.4±21.6	328±176	8.9±4.1	218±131	55.6±10.8
citrate-Ag 30 nm	2.6±0.3	6.2±2.3	19.2±9.3	45.9±22.1	98.4±24.8	31.4±9.0	303±86.0	57.4±33.6
citrate-Ag 70 nm	4.1±2.6	13.0±11.1	19.0±4.8	46.4±28.2	91.9±3.5	42.6±18.0	370±156	35.0±13.2
$AgNO_3$	1.1±0.2	3.0±1.6	n.a.	n.a.	n.a.	0.58±0.11	7.4±1.4	4.0±2.4

IC_{50} – half-inhibitory concentration; bPEI – branched polyethylenimine; PEG – polyethylene glycol; [a] – measured by ICP-MS after the digestion of exposed cells; [b] – measured by ICP-MS after the digestion of exposed and etched cells; * – significant increase of the flow cytometry side scatter signal; n.a. – not available, could not be measured due to toxicity

5.3. The application of antimicrobial and photocatalytic nanoparticles in antimicrobial surface coatings

To address the need for more efficient antimicrobial surfaces, NP-based surface coatings were prepared and ways to improve surface efficiencies were studied. Photocatalytic surfaces induce microbial killing and are able to degrade excess organic matter, therefore photocatalytically active metal oxides were chosen as the primary particle material. Firstly, TiO_2 was chosen to prepare NP-based thin films because TiO_2 is the most known and used photocatalyst[100]. The use of non-dissolvable particles enabled to initially study photocatalysis-driven antibacterial effects without additional complex ion-induced activity. Secondly, the importance of particle dissolution and the high antibacterial effect of Ag^+ ions discussed in the previous chapters was the motivation behind supplementing a dissolvable photocatalytic metal oxide particle (ZnO) with Ag NPs in the following study to combine photocatalytic and ionic effects.

Based on current literature, solution-based synthesis methods are the least energy consuming[113] and therefore, hydrothermal synthesis was used to prepare NP suspensions in both studies. Spin-coating was chosen as a quick and simple method to cover surfaces with the prepared NP suspensions. The prepared surfaces were exposed to UVA-light to initiate photocatalysis-driven effects.

5.3.1. Mechanism of photoinduced toxicity of TiO_2 nanoparticle based thin films (Paper IV)

Suspension of synthesized anatase TiO_2 NPs with hydrodynamic size less than 10 nm was spin-coated onto silicon substrates to prepare ~115 nm thick nano-particulate thin films (Figure 8 A). High specific surface area (150 m^2/g, calculated using particle diameter) ensured the presence of significant amount of surface adsorbed species that can act as electron and/or hole traps[110] thus increasing the efficiency of the photocatalyst by increasing the lifetime of electron-hole pairs.

Time-dependent antibacterial effect of the prepared thin films under UVA-light activation was studied using recombinant bioluminescent *E. coli* as a model microorganism (potential pathogen and sanitary indicator bacterium) for lumine-scence-based assessment of cell viability. The possibility to use long wavelength UV-light (UVA) to activate TiO_2 photocatalysis is a good alternative to direct irradiation of microbes with short wavelength UV-light (UVC) which is germicidal itself but is more harmful to living organisms per se. The applied UVA intensity (22 W/m^2) corresponds to UVA intensity in solar spectrum[138]. The ability of exposed bacteria to form bioluminescent colonies on agarized growth media was determined together with visual inspection of bacterial morphology to evaluate antibacterial effects of UV-treated nano-TiO_2 thin films. After 5 min exposure to UVA on nano-TiO_2 thin films, the colony forming ability of *E. coli*

decreased 4 times and after 20 min exposure no colony forming bacterial cells were detected (Figure 8 B).

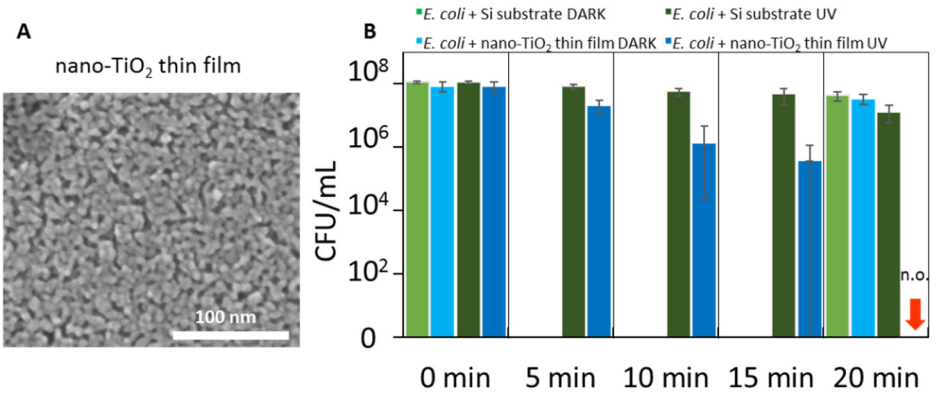

Figure 8. Nano-TiO_2 thin film and colony forming potential of bioluminescent *Escherichia coli* in different exposure conditions. A) SEM image of nano-TiO_2 thin film. B) the effect of UV-irradiation duration on colony forming potential of *E. coli* applied onto Si-monocrystal substrates or nano-TiO_2 thin films. After 20 min of exposure on nano-TiO_2 thin film to UVA light, no viable cells able to grow on agar plate, were observed (marked with n.o. – not observed). The colony forming potential of *E. coli* on surfaces kept in the dark was determined only in the beginning (0 min) and at the end of the experiment (20 min).

As expected, only a slight decrease was seen when *E. coli* was exposed to UVA light on pure silicon control substrates. Bacterial inactivation on TiO_2 thin film after just 20 min UVA exposure was remarkably more effective than in previous studies with similar UVA exposure conditions[139, 140].

Photocatalysis driven morphological changes in bacterial cells were visualised by SEM imaging. SEM imaging revealed that as viable luminescent bacterial number decreased, the shape of bacteria became more expanded and the structure of the bacterial cell membrane was distorted (Figure 9). A halo surrounding the bacteria was observed which might be caused by leakage of organic material from the cell as a result of cell membrane damage. Even though all the bacteria were killed after 20 min UVA exposure, cellular debris was still visible under SEM after 60 min illumination (Paper IV Figure S9). Therefore, it can be suggested that considerably longer time is needed to completely decompose and degrade bacterial cells than the time needed to affect bacterial viability.

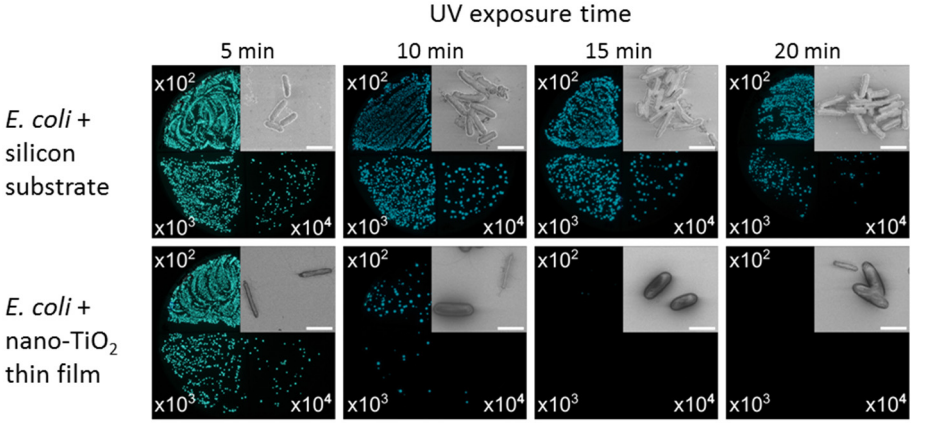

Figure 9. Images of survival of bacteria under UVA-light on control surfaces (upper block of panels) and on nano-TiO_2 thin films (lower block of panels). Different sectors of agar plates show the colonies of luminescent bacteria in 10^2, 10^3 and 10^4-fold dilutions of UV-exposed bacterial suspension. The photos were taken in the dark. Inset on each image is an SEM image of the bacteria after the respective exposure conditions. Scale bars on SEM images correspond to 2 μm.

To elaborate the mechanism of action of nano-TiO_2 thin films UVA-illumination induced changes in chemical structure of the most abundant fatty acids in bacterial plasma membrane (stearic, oleic and linoleic acid)[141–143] were examined by x-ray photoelectron spectroscopy (XPS). It was seen that saturated fatty acid (stearic acid) directly degraded during UVA exposure, but unsaturated fatty acids (oleic and linoleic acid) went through changes in their chemical composition before total degradation (Paper IV Figure 3). Although photo-oxidation of the three fatty acids passed several stages, the time required for total photo-degradation (10 min) was similar for them all. It has been shown that cell membrane susceptibility to TiO_2 photo-oxidation can be linked to the degree of unsaturation of fatty acid chains of phospholipids[108, 144]. Our study suggested that the loss of integrity of the main cellular outer barriers and bacterial envelope is the cause for antibacterial effect of photo-activated nano-TiO_2 thin film. Our statement is in agreement with a report by Kubacka et al.[101] showing the importance of cell wall and cell membrane related biological processes in the antibacterial activity of TiO_2 NP containing thin films.

5.3.2. Antimicrobial effect of ZnO and ZnO/Ag composite nanoparticle covered surfaces (Paper V)

A well-known and widely used photocatalyst besides TiO_2 is ZnO. Nanosized ZnO is partially soluble and the released Zn^{2+}-ions are known to have antimicrobial properties[102]. Thus, ZnO was chosen as an ion-releasing photocatalytic metal oxide material to prepare NP covered photocatalytic and antimicrobial

surfaces. Ag was photodeposited onto ZnO particles to increase photocatalytic efficacy by acting as an electron sink and therefore prolonging electron-hole pair lifetime[145–147]. Zn^{2+} and Ag^{+} ions are both known for their antimicrobial effect and therefore the prepared NP covered surfaces were expected to have a combined effect of increased photocatalysis and released metal ions.

Well-defined and clearly separated ~80x30 nm rod-like ZnO particles were synthesized using hydrothermal method. ZnO particles were stabilized in butanol using acac and Ag was photodeposited onto ZnO particles using UVA illumination. Ag concentrations were chosen on the basis of previous research on ZnO/Ag composite particles[115, 116, 145, 146, 148–150]. The morphology of ZnO and ZnO/Ag composite particles was similar according to TEM. STEM-EDX analysis revealed silver depositions on ZnO particles (Figure 10 A). UV-Vis measurements of suspensions demonstrated localized surface plasmon resonance peak at ~425 nm which is characteristic to Ag NPs[151] (Figure 10 B). XRD analysis showed the presence of crystalline ZnO[148]. Ag structure was not detected with XRD which might be because of the very low amount of Ag or amorphous phase of Ag (Paper V Figure S3). Aliquots of ZnO or ZnO/Ag composite NP suspensions were applied to glass substrates by spin-coating to prepare particle covered surfaces. It is noteworthy that NP covered surfaces (immobilized NPs) have been significantly less studied for their antimicrobial activity than NPs in the form of a suspension.

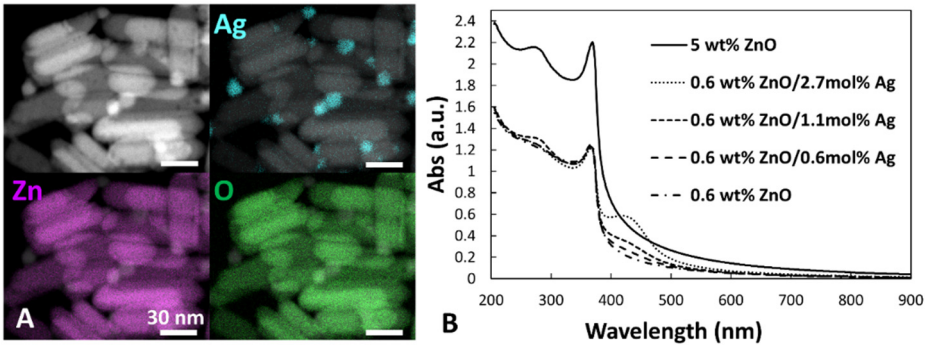

Figure 10. Characterization of ZnO and ZnO/Ag NPs in STEM, EDX and UV-Vis. A: HAADF- STEM images and EDX mapping of ZnO/Ag composite NPs. HAADF-STEM images combined with EDX mapping results show silver (Ag) L_α in blue, zinc (Zn) K_α in violet and oxygen (O) K_α in green. Scale bars correspond to 30 nm. B: UV-Vis absorbance spectra of ZnO and ZnO/Ag composite NP suspensions. Surface plasmon resonance peak at ~425 nm is characteristic to Ag NPs.

Two different surface coverage densities were used to evaluate the influence of the amount of ZnO on the surface. Three concentrations of Ag were chosen to evaluate the influence of Ag on photocatalytic and antimicrobial effect. The surfaces contained either 2 µg Zn (in the form of ZnO) and 0, 0.005, 0.014 or 0.022 µg Ag (sparse coverage) or 20 µg Zn (in the form of ZnO) (dense coverage)

per cm^2. SEM indicated even coverage of ZnO particles on all prepared surfaces and no visual difference between pure ZnO and Ag supplemented ZnO covered surfaces was seen (Figure 11). Photodegradation of model dye by all NP suspensions was characterized to check the influence of added Ag deposits on photocatalytic activity. The most remarkable increase compared to pure ZnO was seen with composite particles with the highest silver content (Figure 12 A). It has been claimed that the observed increase is the result of added Ag acting as an electron sink and prolonging the lifetime of electron-hole pairs. Photodegradation of dye also depended on ZnO concentration as was expected (Figure 12 B).

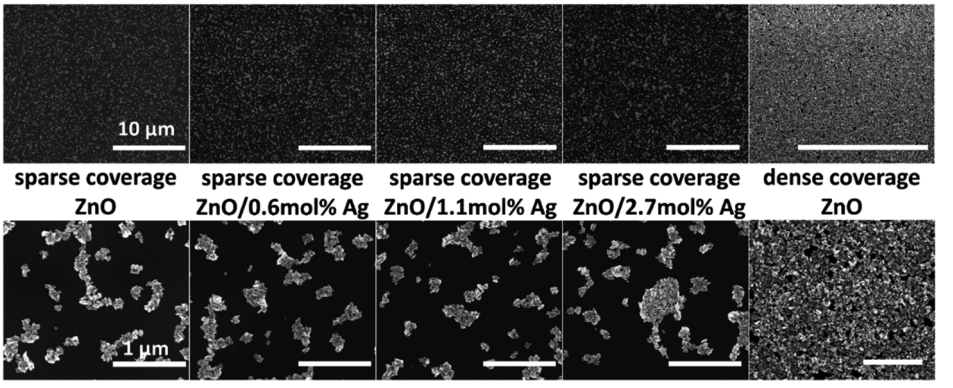

Figure 11. SEM images of ZnO and ZnO/Ag composite NP covered surfaces. Scale bars correspond to 10 µm (upper panels) or 1 µm (lower panels).

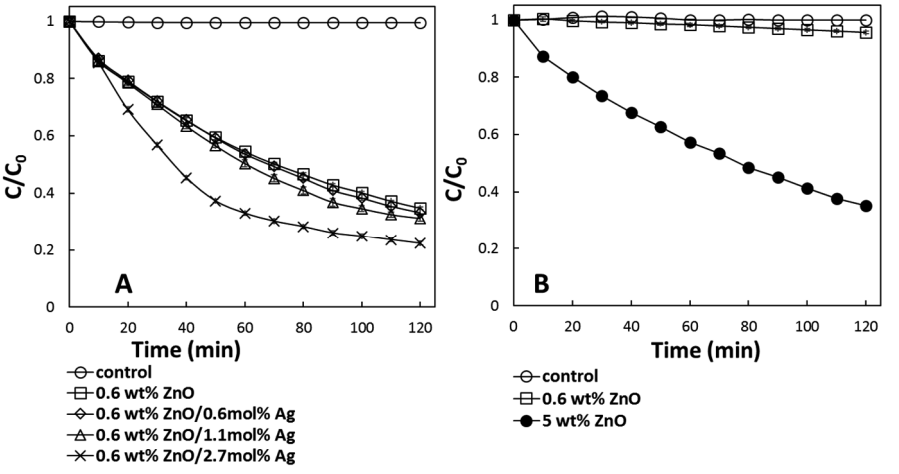

Figure 12. Photocatalytic activity of ZnO and ZnO/Ag NPs under UVA irradiation. A: 0.6 wt% ZnO and ZnO/Ag composite NP suspensions and B: 10× more diluted suspensions compared to A of 0.6 and 5 wt% ZnO NPs; all suspensions were in butanol with model dye. Control – model dye (brilliant blue FCF) solution. Graphs represent averages and standard deviations (due to small values not visible on the graphs) of three

experiments. X-axis – UVA irradiation time (min). Y-axis – change in absorbance of model dye at characteristic wavelength (630 nm) (C/C_0).

For antimicrobial activity testing of the prepared surfaces, improved test protocol was developed based on ISO 27447:2009 for higher throughput. Our modified test protocol enabled quantification of the decrease in viable microbial counts by three logs and therefore fulfils the requirement for 99.9% decrease of microbes on surfaces as required by the US standards but does not allow the assessment of 4–5 log decrease as required by the EN standards for surfaces in healthcare settings. Three model pathogenic organisms were used: *E. coli*, *S. aureus* and *C. albicans*. Antimicrobial efficiency of our ZnO and ZnO/Ag surfaces in the dark was relatively small (Figure 13 A, C and E). Though, after 60 min incubation the toxic effect of ZnO covered surfaces became statistically relevant (Paper V Figure 5). Also, sparse coverage ZnO surface with the highest Ag content showed significant effect in the dark causing >3 log reduction of *E. coli* and *S. aureus* after 60 min incubation (Figure 13 A and C). In the applied test conditions, *S. aureus* seemed to be more sensitive to surfaces-induced effects than *E. coli*. *C. albicans* was the least sensitive.

Surfaces were notably more effective under UVA illumination (Figure 13 B, D, F). UV-induced antimicrobial activity of surfaces was dependent on ZnO content. Dense coverage ZnO surfaces enabled ~2 log reduction of viable bacterial cells already after 15 min incubation and can be considered very efficient. Further incubation resulted in reduction of viable counts exceeding our limit of quantification. For practical application, short killing times are preferred and therefore 24 h incubation time required in the current standards has been criticized[97]. The addition of Ag to ZnO generally increased antimicrobial activity. The effect of the surfaces with the highest Ag content was the most significant and after less than 30 min illumination resulted in >3 log reduction of viable bacteria. The effect was the lowest for *C. albicans*, likely due to higher resistance of fungal cells[152] and only 0.6 log reduction occurred after 60 min incubation.

Our tests showed that NPs were not released from the surfaces during the exposures, therefore in addition to photocatalytic activity, only released ionic Zn and Ag can add to antimicrobial efficiency. We exposed bacterial cells to Zn^{2+} ion (from soluble $ZnSO_4$) concentrations which corresponded to the amounts of ions released from the surface (determined by dissolution experiments) (Paper V Figure S5) to study the influence of Zn^{2+} ions on overall toxicity. No toxicity was seen toward *S. aureus* and *C. albicans*. However, significant dose-independent effect was observed for *E. coli*. *S. aureus* has been shown to be less susceptible to Ag-ZnO treatment than *E. coli*, probably due to weaker antioxidant cellular content of *E. coli* that renders the latter less resistant to oxidative stress[153, 154]. Comparison of toxicity of surfaces with ionic toxicity also showed difference between *E. coli* and the other two test organisms. Thus, for *E. coli* it would be plausible to explain surface toxicity with the release of metal ions or oxidative stress. However, ZnO surfaces were lacking dose effect in the dark but had a clear dose-dependent difference under UVA which confirms photocatalysis as the main contributor to the antimicrobial effect.

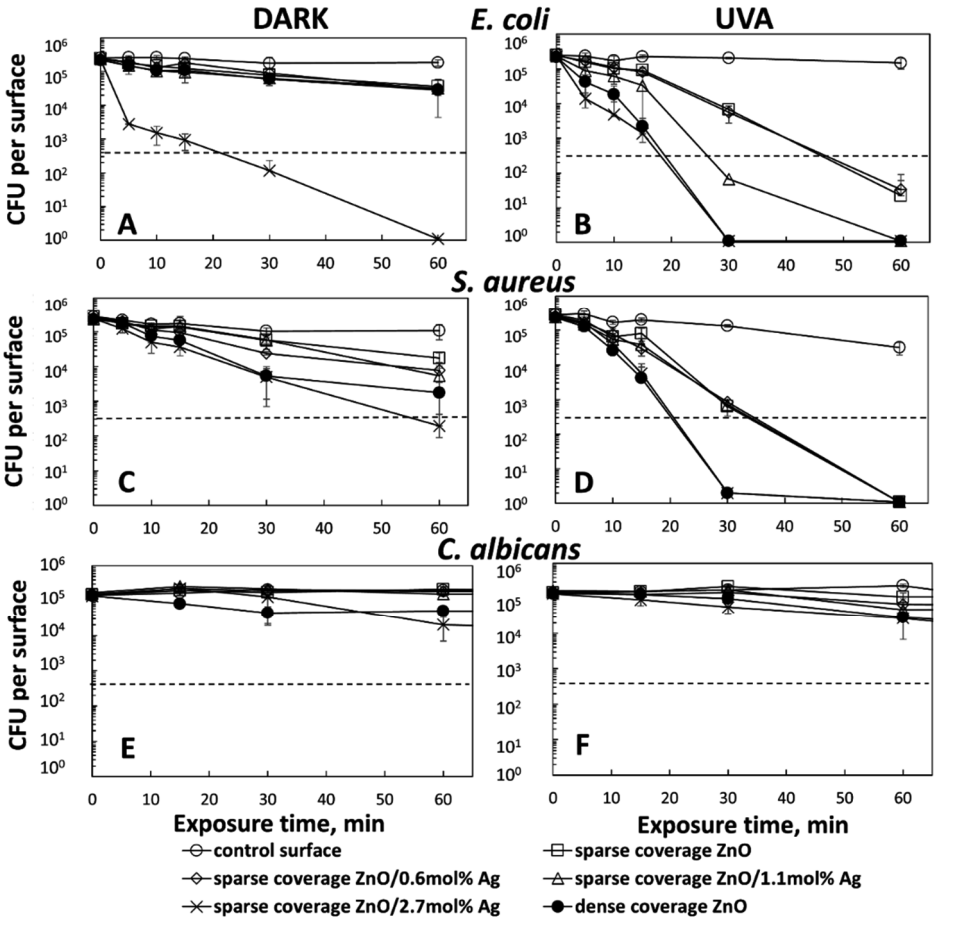

Figure 13. Viability of microorganisms on ZnO and ZnO/Ag surfaces in the dark and under UVA illumination. Viability of *Escherichia coli* (A and B), *Staphylococcus aureus* (C and D), *Candida albicans* (E and F) exposed to ZnO and ZnO/Ag composite NP covered surfaces, expressed in colony forming units (CFU). Left – surfaces kept in the dark as control. Right – UVA exposed surfaces. Graphs represent averages and standard deviations of three experiments. Dotted line: limit of quantification for CFUs.

Increased photocatalytic activity in the case of higher amount of ZnO or increased Ag content in ZnO/Ag composites was as well confirmed by model dye photo-degradation test (Figure 12). Other previously published papers have reported that ROS[155–157] and slow release of metal ions[158] are the main mechanisms driving the toxicity of ZnO/Ag containing materials. We observed relatively low release of Zn^{2+} ions from our surfaces even under UVA illumination. As these concentrations were not toxic for *S. aureus* and *C. albicans*, we suggest the possibility for additional local release of Zn near cell walls[159]. Our study didn't involve testing of ROS production and therefore further research is needed to clearly distinguish

between effects caused by the ions and ROS. Photodegradation of membrane associated fatty acids is probably also occurring as was shown in Paper IV.

For practical applications, the reusability of antimicrobial surfaces is extremely important. We tested the antibacterial efficacy of sparse coverage ZnO surfaces with the highest Ag content during 10 usage cycles. Although TXRF and AAS analysis showed decreased Zn and Ag content of the surfaces after usage cycles, we didn't observe significant decrease in neither antibacterial activity (Paper V Figure 7) nor photodegradation capability of the surface (Paper V Figure S7). According to our knowledge, our study is the first to demonstrate the reusability of ZnO/Ag surfaces for antimicrobial applications. The use of Ag NPs showed increased photocatalytic and antimicrobial activity even in very low concentrations (0.005, 0.014 or 0.022 µg Ag per cm^2) and therefore, ZnO/Ag combination can be considered a perspective material in antimicrobial coatings.

CONCLUSIONS

Novel properties of nanosized materials are exploited in numerous consumer products and in product development. The increased interest in the use of nanomaterials (NMs) has created a need for better understanding of their influence on relevant organisms. The most widely used NMs in consumer products are silver nanoparticles (Ag NPs) and the respective applications mainly exploit the antimicrobial nature of Ag. In addition to favorable properties, the newly developed NMs may induce unwanted effects towards non-target organisms. The main aim of the current study was to design novel antimicrobial Ag NP-containing surfaces. Therefore, the current thesis includes studies about the toxicity and the mechanism of toxicity of a library of Ag NPs towards microbial and mammalian cells and the use of NPs in antimicrobial coatings. The focus has been on understanding the influence of particle physico-chemical properties on their antimicrobial activity and toxicity towards mammalian cells to be able to recommend the use of the most adequate materials in antimicrobial product development. The possible application of NPs in antimicrobial coatings was studied as that field of NP use has been under constant increased interest.

The thesis showed that in the case of rather large Ag NPs (~80 nm in diameter) the effect towards model bacterium *Escherichia coli* was not shape-dependent (nanospheres vs nanowires) and could be fully explained by particle dissolution and bioavailability of Ag^+ ions. A library of variously sized spherical Ag particles (10, 20, 30, 40, 60, 70 and 80 nm) was studied and increased antimicrobial activity and toxicity with decreasing particle size was observed. It was seen that Ag particles were ~10 times less toxic to mammalian cells than to bacterial cells and the effect towards mammalian cells was explained by the release of Ag^+ ions. For 20 nm to 80 nm Ag NPs, the size-dependent antimicrobial activity was explained by increased particle dissolution but the effect of 10 nm particles couldn't be explained by abiotic dissolved Ag. The nano-specific effect of 10 nm particles was further studied and it was confirmed that increased bioavailability of Ag^+ ions was the reason for increased antimicrobial efficacy. Although the mechanism of increased bioavailability of Ag^+ ions from 10 nm Ag particles is not clear, it is hypothesized to arise from processes happening in close vicinity of the cell. As overall particle dissolution in abiotic conditions does not always explain the complex mechanism of Ag biological effects, additional research is needed to clarify the mechanism of influence.

In addition to particle shape and size it is important to understand the influence of particle surface charge on toxicity as different particle coatings are used in various applications. The effect of a library of Ag particles with different surface coatings (branched polyethylenimine, citrate, polyethylene glycol) and subsequently different surface charges (positive, negative, near-neutral) towards mammalian cells was studied. NP-cell interactions were studied to explain the mechanism through which Ag particles influence the cells. Positively charged particles were seen to cause higher cytotoxicity and bind to cells more effectively

than particles with negative and neutral surface charge. Cell-bound and intracellular Ag was quantitatively distinguished from each other and comparable intracellular Ag concentrations were observed at half maximal inhibitory concentrations of all the particles. This suggests that internalization capability of particles significantly influences their cytotoxicity.

As the spread of multidrug resistant microbes has raised the need for new antimicrobial treatments, the current thesis addressed the issue of NP-based antimicrobial surfaces. Photocatalytic material-based NP covered surfaces were prepared as photocatalysis is known to result in degradation of organic matter including microbes. First, non-soluble photocatalytic NPs (TiO_2) were prepared and coated onto substrates by spin-coating to understand the mechanisms through which immobilized photocatalytic NPs cause antibacterial activity. SEM imaging confirmed that damages to bacterial cell envelope occur in the same time frame as bacterial inactivation in the viability study. Decomposition of common fatty acids of bacterial plasma membrane was suggested to be the reason for morphological changes and leakage of bacterial cell components that was observed in SEM. Next, the use of Ag NPs in combination with ion-releasing photocatalytic NPs (ZnO) was studied to understand the influence of Ag on photocatalytic activity and to develop highly efficient coatings based on a combined effect of photocatalysis and antimicrobial ions. High efficiency was expected as both materials were ion-releasing and both ions (Zn^{2+}, Ag^{+}) are known to have antimicrobial activity. The developed ZnO/Ag NP-based coatings showed high antimicrobial activity however a straightforward ionic effect towards the studied microbes (bacteria, fungi) was not proven. The observed effect was potentially mostly photocatalysis-driven.

Reusability of the prepared surfaces was tested and no significant decrease in neither antibacterial activity nor photodegradation capability was observed after 10 usage cycles. According to our knowledge, our study was the first to demonstrate the reusability of ZnO/Ag surfaces for antimicrobial applications. Altogether it was shown that the addition of Ag increased photocatalytic effect and antimicrobial efficiency of the prepared surfaces and therefore Ag can be considered a suitable material to increase the efficiency of photocatalytic material-based antimicrobial coatings.

Results of the present thesis support the use of Ag NPs in combination with photocatalytic NPs to prepare efficient antimicrobial coatings that in addition to microbial killing also potentially degrade surface contaminating organic matter (including microbes). In addition, the results suggest avoiding the use of positively charged Ag NPs in human directed products as cationic particles presented notably higher toxic effect to mammalian cells.

SUMMARY IN ESTONIAN

Metalliliste nanoosakeste disain ja füüsikalis-keemiline iseloomustamine ning nende rakendamine antimikroobsetes pinnakatetes

Uudsete omadustega nanosuuruses materjale rakendatakse arvukates tarbekaupades ning tootearenduses. Suurenenud huvi nanomaterjalide kasutuse vastu on tekitanud vajaduse paremini aru saada nende mõjust ümbritsevale, sest lisaks soovitud omadustele võivad need esile kutsuda soovimatuid mõjusid mittesihtorganismidele. Tarbekaupades enimkasutatud nanomaterjal on hõbe (edaspidi Ag) ning peamiselt rakendatakse toodetes Ag antimikroobset toimet.

Käesoleva dissertatsiooni peamiseks eesmärgiks oli disainida Ag nanoosakesi sisaldavad uudsed antimikroobsed, ent mitte-sihtorganismidele (sh inimestele) ohutud pinnakatted. Soovitamaks antimikroobsete toodete arenduseks kõige sobivamaid materjale, uuriti Ag, TiO_2 ja ZnO nanoosakeste antimikroobset toimet ning mürgisust imetajarakkudele, nanoosakeste füüsikalis-keemiliste omaduste mõju antimikroobsusele ja mürgisusele ning toimemehhanisme.

Antud tööst selgub, et suurte Ag nanoosakeste puhul (~80 nm läbimõõduga) ei sõltu nende toime mudelbakterile *Escherichia coli* osakese kujust (nanosfäärid vs nanotraadid), vaid on täielikult seletatav osakese lahustuvuse ja Ag^+ ioonide biosaadavusega. Erineva suurusega (10, 20, 30, 40, 60, 70 ja 80 nm) sfääriliste Ag osakeste puhul leiti, et osakese suuruse vähenedes suurenes nende antimikroobne toime ja mürgisus. Leiti, et Ag osakesed olid imetajarakkudele ~10 korda vähem mürgised kui bakteritele ning mõju imetajarakkudele oli seletatav vabanenud Ag^+ ioonidega. 20–80 nm läbimõõduga osakeste puhul oli osakese suurusest sõltuv antibakteriaalne toime samuti seletatav suurenenud lahustuvusega. Sama järeldus ei kehtinud 10 nm osakeste puhul ning edasised uuringud näitasid, et 10 nm osakeste suurenenud antibakteriaalsus tulenes Ag^+ ioonide suurenenud biosaadavusest, mis eeldatavalt tuleneb bakteriraku piirpinnal toimuvatest protsessidest. Ag osakeste keerukat mõjumehhanismi uurides peab seega arvestama, et abiootilistes tingimustes mõõdetud osakese lahustuvus ei pruugi täielikult seletada osakese mürgisust bakteritele ning mõjumehhanismi selgitamiseks on vajalikud täiendavad uuringud.

Kuna rakendustes kasutatakse erineva kattega osakesi, on lisaks osakese kujule ja suurusele oluline mõista ka pinnalaengu mõju mürgisusele. Kirjeldatud mõju selgitamiseks uuriti erinevalt kaetud (hargnenud polüetüleenimiin, tsitraat, polüetüleenglükool) ning sellest tulenevalt erineva pinnalaenguga (positiivne, negatiivne, neutraalse-lähedane) Ag nanoosakeste mõju imetajarakkudele. Kaasnevate mõjumehhanismide selgitamiseks uuriti nanoosakeste ja rakkude vahelisi vastasmõjusid. Võrreldes negatiivselt ja neutraalse-lähedaselt laetud osakestega täheldati positiivse pinnalaenguga osakeste puhul suurenenud mürgisust ja efektiivsemat imetajarakuga seondumist. Rakumembraaniga seondunud ja rakusisest Ag-d eristati kvantitatiivselt ning näidati, et kõikide osakeste puhul oli

keskmiselt pärssiva kontsentratsiooni juures rakusisese Ag kogus sarnane. Nähtu põhjal võib eeldata, et osakeste rakku sisenemise võime mõjutab märkimisväärselt nende mürgisust ning positiivse pinnalaenguga osakesed mõjuvad imetajarakkudele oluliselt mürgisemalt.

Multiresistentsete mikroobide levik on tekitanud vajaduse uudsete antimikroobsete toodete järele ning seepärast tegeles käesolev dissertatsioon nanoosakestel põhinevate antimikroobsete pindadega. Fotokatalüüsi käigus lagundatakse orgaanilist ainet, sealhulgas mikroobe, ning seepärast kasutati pindade katmiseks fotokatalüütilisi nanoosakesi. Esmalt valmistati immobiliseeritud fotokatalüütiliste nanoosakeste antibakteriaalsuse mehhanismide uurimiseks vurrkatmise teel mittelahustuvate fotokatalüütiliste osakestega (TiO_2) kaetud pinnad. Skaneeriva elektronmikroskoopia (SEM) uuringud kinnitasid, et kahjustused bakterite kestale ilmnesid samaaegselt elumuse uuringus nähtud bakterite inaktiveerumisega. SEMi uuringus nähtud bakterikesta morfoloogiliste muutuste ja bakteriraku sisu lekkimise põhjuseks oli oletatavalt bakteri plasmamembraanis sisalduvate rasvhapete lagunemine. Järgnevalt uuriti Ag nanoosakeste koosmõju lahustuvate fotokatalüütiliste nanoosakestega (ZnO), et mõista Ag mõju fotokatalüüsi aktiivsusele ja arendada fotokatalüüsi ja antimikroobsete ioonide koosmõjus suure efektiivsusega pinnakatteid. Suure antimikroobse efektiivsuse eeldus oli mõlema materjali osaline lahustuvus ning Zn^{2+} ja Ag^{+} ioonide antimikroobsed omadused. ZnO/Ag nanoosakestel põhinevad pinnakatted olid kõrge antimikroobse efektiivsusega, kuid otsest ioonidest tulenevat efekti uuritud mikroobidele (bakterid, pärmseen) ei tõestatud. Nähtud mõju näis põhiliselt tulenevat fotokatalüüsist.

Väljatöötatud pinnakatete korduvkasutatavuse hindamine näitas, et pinnakatete antibakteriaalne aktiivsus ja fotokatalüütilise lagundamise võime ei vähenenud märkimisväärselt ka pärast kümmet kasutustsüklit. Meile teadaolevalt oli meie uurimus esimene, mis näitas ZnO/Ag pindade korduvkasutatavust antimikroobses rakenduses. Kokkuvõtvalt näidati, et Ag lisamine suurendas pindade fotokatalüütilist ja antimikroobset mõju ning seepärast on Ag sobiv fotokatalüütilistel materjalidel põhinevate antimikroobsete pinnakatete efektiivsuse suurendamiseks.

Käesoleva dissertatsiooni tulemused toetavad Ag nanoosakeste kombineerimist fotokatalüütiliste materjalidega efektiivsete antimikroobsete ning orgaanilist ainet (sh mikroobe) lagundavate pinnakatete valmistamisel. Ühtlasi võib saadud tulemuste põhjal soovitada positiivse pinnalaenguga Ag nanoosakeste kasutamise vältimist toodetes, millega inimene vahetult kokku puutub, sest sellised osakesed olid imetajarakkudele märkimisväärselt mürgisemad kui negatiivse või neutraalse laenguga osakesed.

REFERENCES

1. Kreyling, W. G.; Semmler-Behnke, M.; Chaudhry, Q., A complementary definition of nanomaterial. *Nano Today* **2010,** *5* (3), 165–168.
2. Bleeker, E. A. J.; de Jong, W. H.; Geertsma, R. E.; Groenewold, M.; Heugens, E. H. W.; Koers-Jacquemijns, M.; van de Meent, D.; Popma, J. R.; Rietveld, A. G.; Wijnhoven, S. W. P.; Cassee, F. R.; Oomen, A. G., Considerations on the EU definition of a nanomaterial: Science to support policy making. *Regulatory Toxicology and Pharmacology* **2013,** *65* (1), 119–125.
3. European Commission Recommendation of 18 October 2011 on the definition of nanomaterial (2011/696/EU). 2011.
4. Oberdörster, G.; Oberdörster, E.; Oberdörster, J., Nanotoxicology: An emerging discipline evolving from studies of ultrafine particles. *Environmental Health Perspectives* **2005,** *113* (7), 823–839.
5. Law, M.; Greene, L. E.; Johnson, J. C.; Saykally, R.; Yang, P. D., Nanowire dye-sensitized solar cells. *Nature Materials* **2005,** *4* (6), 455–459.
6. Wiley, B.; Sun, Y. G.; Xia, Y. N., Synthesis of silver nanostructures with controlled shapes and properties. *Accounts of Chemical Research* **2007,** *40* (10), 1067–1076.
7. Hu, L. B.; Kim, H. S.; Lee, J. Y.; Peumans, P.; Cui, Y., Scalable Coating and Properties of Transparent, Flexible, Silver Nanowire Electrodes. *ACS Nano* **2010,** *4* (5), 2955–2963.
8. Wang, X. Y.; Zhang, L.; Wang, J. Q.; Liu, X.; Lv, P.; Zeng, J.; Liu, G., Size-Controlled Biocompatible Silver Nanoplates for Contrast-Enhanced Intravital Photoacoustic Mapping of Tumor Vasculature. *Journal of Biomedical Nanotechnology* **2018,** *14* (8D), 1448–1457.
9. Vance, M. E.; Kuiken, T.; Vejerano, E. P.; McGinnis, S. P.; Hochella, M. F.; Rejeski, D.; Hull, M. S., Nanotechnology in the real world: Redeveloping the nanomaterial consumer products inventory. *Beilstein Journal of Nanotechnology* **2015,** *6*, 1769–1780.
10. Kahru, A.; Ivask, A., Mapping the Dawn of Nanoecotoxicological Research. *Accounts of Chemical Research* **2013,** *46* (3), 823–833.
11. Choi, J.-Y.; Ramachandran, G.; Kandlikar, M., The Impact of Toxicity Testing Costs on Nanomaterial Regulation. *Environmental Science & Technology* **2009,** *43* (9), 3030–3034.
12. Bondarenko, O.; Juganson, K.; Ivask, A.; Kasemets, K.; Mortimer, M.; Kahru, A., Toxicity of Ag, CuO and ZnO nanoparticles to selected environmentally relevant test organisms and mammalian cells in vitro: a critical review. *Archives of Toxicology* **2013,** *87* (7), 1181–1200.
13. Colman, B. P.; Arnaout, C. L.; Anciaux, S.; Gunsch, C. K.; Hochella, M. F.; Kim, B.; Lowry, G. V.; McGill, B. M.; Reinsch, B. C.; Richardson, C. J.; Unrine, J. M.; Wright, J. P.; Yin, L. Y.; Bernhardt, E. S., Low Concentrations of Silver Nanoparticles in Biosolids Cause Adverse Ecosystem Responses under Realistic Field Scenario. *PLOS ONE* **2013,** *8* (2).
14. Piccinno, F.; Gottschalk, F.; Seeger, S.; Nowack, B., Industrial production quantities and uses of ten engineered nanomaterials in Europe and the world. *Journal of Nanoparticle Research* **2012,** *14* (9).
15. Ivask, A.; Juganson, K.; Bondarenko, O.; Mortimer, M.; Aruoja, V.; Kasemets, K.; Blinova, I.; Heinlaan, M.; Slaveykova, V.; Kahru, A., Mechanisms of toxic action

of Ag, ZnO and CuO nanoparticles to selected ecotoxicological test organisms and mammalian cells in vitro: A comparative review. *Nanotoxicology* **2014,** *8*, 57–71.
16. Nel, A.; Xia, T.; Madler, L.; Li, N., Toxic potential of materials at the nanolevel. *Science* **2006,** *311* (5761), 622–627.
17. Li, W. R.; Xie, X. B.; Shi, Q. S.; Zeng, H. Y.; Ou-Yang, Y. S.; Chen, Y. B., Antibacterial activity and mechanism of silver nanoparticles on Escherichia coli. *Applied Microbiology and Biotechnology* **2010,** *85* (4), 1115–1122.
18. Sondi, I.; Salopek-Sondi, B., Silver nanoparticles as antimicrobial agent: a case study on E-coli as a model for Gram-negative bacteria. *Journal of Colloid and Interface Science* **2004,** *275* (1), 177–182.
19. Morones, J. R.; Elechiguerra, J. L.; Camacho, A.; Holt, K.; Kouri, J. B.; Ramirez, J. T.; Yacaman, M. J., The bactericidal effect of silver nanoparticles. *Nanotechnology* **2005,** *16* (10), 2346–2353.
20. Xiu, Z. M.; Zhang, Q. B.; Puppala, H. L.; Colvin, V. L.; Alvarez, P. J. J., Negligible Particle-Specific Antibacterial Activity of Silver Nanoparticles. *Nano Letters* **2012,** *12* (8), 4271–4275.
21. Bondarenko, O.; Ivask, A.; Käkinen, A.; Kurvet, I.; Kahru, A., Particle-Cell Contact Enhances Antibacterial Activity of Silver Nanoparticles. *PLOS ONE* **2013,** *8* (5).
22. Ivask, A.; ElBadawy, A.; Kaweeteerawat, C.; Boren, D.; Fischer, H.; Ji, Z.; Chang, C. H.; Liu, R.; Tolaymat, T.; Telesca, D.; Zink, J. I.; Cohen, Y.; Holden, P. A.; Godwin, H. A., Toxicity Mechanisms in Escherichia coli Vary for Silver Nanoparticles and Differ from Ionic Silver. *ACS Nano* **2014,** *8* (1), 374–386.
23. Kumar, A.; Pandey, A. K.; Singh, S. S.; Shanker, R.; Dhawan, A., Cellular uptake and mutagenic potential of metal oxide nanoparticles in bacterial cells. *Chemosphere* **2011,** *83* (8), 1124–1132.
24. Pareek, V.; Gupta, R.; Panwar, J., Do physico-chemical properties of silver nanoparticles decide their interaction with biological media and bactericidal action? A review. *Materials Science & Engineering: C Materials for Biological Applications* **2018,** *90*, 739–749.
25. Feng, Q. L.; Wu, J.; Chen, G. Q.; Cui, F. Z.; Kim, T. N.; Kim, J. O., A mechanistic study of the antibacterial effect of silver ions on Escherichia coli and Staphylococcus aureus. *Journal of Biomedical Materials Research* **2000,** *52* (4), 662–668.
26. Lok, C. N.; Ho, C. M.; Chen, R.; He, Q. Y.; Yu, W. Y.; Sun, H.; Tam, P. K. H.; Chiu, J. F.; Che, C. M., Silver nanoparticles: partial oxidation and antibacterial activities. *Journal of Biological Inorganic Chemistry* **2007,** *12* (4), 527–534.
27. Kim, J. S.; Kuk, E.; Yu, K. N.; Kim, J. H.; Park, S. J.; Lee, H. J.; Kim, S. H.; Park, Y. K.; Park, Y. H.; Hwang, C. Y.; Kim, Y. K.; Lee, Y. S.; Jeong, D. H.; Cho, M. H., Antimicrobial effects of silver nanoparticles. *Nanomedicine: Nanotechnology, Biology and Medicine* **2007,** *3* (1), 95–101.
28. Zhao, F.; Zhao, Y.; Liu, Y.; Chang, X. L.; Chen, C. Y.; Zhao, Y. L., Cellular Uptake, Intracellular Trafficking, and Cytotoxicity of Nanomaterials. *Small* **2011,** *7* (10), 1322–1337.
29. Kafshgari, M. H.; Harding, F. J.; Voelcker, N. H., Insights into Cellular Uptake of Nanoparticles. *Current Drug Delivery* **2015,** *12* (1), 63–77.
30. Jiang, X.; Miclaus, T.; Wang, L.; Foldbjerg, R.; Sutherland, D. S.; Autrup, H.; Chen, C.; Beer, C., Fast intracellular dissolution and persistent cellular uptake of silver nanoparticles in CHO-K1 cells: implication for cytotoxicity. *Nanotoxicology* **2015,** *9* (2), 181–189.

31. Shin, S. W.; Song, I. H.; Um, S. H., Role of Physicochemical Properties in Nanoparticle Toxicity. *Nanomaterials* **2015,** *5* (3), 1351–1365.
32. Gliga, A. R.; Skoglund, S.; Wallinder, I. O.; Fadeel, B.; Karlsson, H. L., Size-dependent cytotoxicity of silver nanoparticles in human lung cells: the role of cellular uptake, agglomeration and Ag release. *Particle and Fibre Toxicology* **2014,** *11*.
33. Birben, E.; Sahiner, U. M.; Sackesen, C.; Erzurum, S.; Kalayci, O., Oxidative stress and antioxidant defense. *The World Allergy Organization Journal* **2012,** *5* (1), 9–19.
34. Kim, H. R.; Kim, M. J.; Lee, S. Y.; Oh, S. M.; Chung, K. H., Genotoxic effects of silver nanoparticles stimulated by oxidative stress in human normal bronchial epithelial (BEAS-2B) cells. *Mutation Research-Genetic Toxicology and Environmental Mutagenesis* **2011,** *726* (2), 129–135.
35. Manke, A.; Wang, L. Y.; Rojanasakul, Y., Mechanisms of Nanoparticle-Induced Oxidative Stress and Toxicity. *BioMed Research International* **2013,** 942916.
36. Chairuangkitti, P.; Lawanprasert, S.; Roytrakul, S.; Aueviriyavit, S.; Phummiratch, D.; Kulthong, K.; Chanvorachote, P.; Maniratanachote, R., Silver nanoparticles induce toxicity in A549 cells via ROS-dependent and ROS-independent pathways. *Toxicology in Vitro* **2013,** *27* (1), 330–338.
37. Dakal, T. C.; Kumar, A.; Majumdar, R. S.; Yadav, V., Mechanistic Basis of Antimicrobial Actions of Silver Nanoparticles. *Frontiers in Microbiology* **2016,** *7*.
38. Nel, A. E.; Brinker, C. J.; Parak, W. J.; Zink, J. I.; Chan, W. C. W.; Pinkerton, K. E.; Xia, T.; Baer, D. R.; Hersam, M. C.; Weiss, P. S., Where Are We Heading in Nanotechnology Environmental Health and Safety and Materials Characterization? *ACS Nano* **2015,** *9* (6), 5627–5630.
39. Rasmussen, K.; Rauscher, H.; Mech, A.; Sintes, J. R.; Gilliland, D.; Gonzalez, M.; Kearns, P.; Moss, K.; Visser, M.; Groenewold, M.; Bleeker, E. A. J., Physicochemical properties of manufactured nanomaterials – Characterisation and relevant methods. An outlook based on the OECD Testing Programme. *Regulatory Toxicology and Pharmacology* **2018,** *92*, 8–28.
40. Fadeel, B.; Fornara, A.; Toprak, M. S.; Bhattacharya, K., Keeping it real: The importance of material characterization in nanotoxicology. *Biochemical and Biophysical Research Communications* **2015,** *468* (3), 498–503.
41. Djurisic, A. B.; Leung, Y. H.; Ng, A. M. C.; Xu, X. Y.; Lee, P. K. H.; Degger, N.; Wu, R. S. S., Toxicity of Metal Oxide Nanoparticles: Mechanisms, Characterization, and Avoiding Experimental Artefacts. *Small* **2015,** *11* (1), 26–44.
42. Laborda, F.; Bolea, E.; Cepria, G.; Gomez, M. T.; Jimenez, M. S.; Perez-Arantegui, J.; Castillo, J. R., Detection, characterization and quantification of inorganic engineered nanomaterials: A review of techniques and methodological approaches for the analysis of complex samples. *Analytica Chimica Acta* **2016,** *904*, 10–32.
43. Martinez-Castanon, G. A.; Nino-Martinez, N.; Martinez-Gutierrez, F.; Martinez-Mendoza, J. R.; Ruiz, F., Synthesis and antibacterial activity of silver nanoparticles with different sizes. *Journal of Nanoparticle Research* **2008,** *10* (8), 1343–1348.
44. Lu, Z.; Rong, K. F.; Li, J.; Yang, H.; Chen, R., Size-dependent antibacterial activities of silver nanoparticles against oral anaerobic pathogenic bacteria. *Journal of Materials Science: Materials in Medicine* **2013,** *24* (6), 1465–1471.
45. Bowman, C. R.; Bailey, F. C.; Elrod-Erickson, M.; Neigh, A. M.; Otter, R. R., Effects of silver nanoparticles on zebrafish (Danio rerio) and Escherichia coli (ATCC 25922): A comparison of toxicity based on total surface area versus mass concentration of particles in a model eukaryotic and prokaryotic system. *Environmental Toxicology and Chemistry* **2012,** *31* (8), 1793–1800.

46. Wang, X.; Ji, Z.; Chang, C. H.; Zhang, H.; Wang, M.; Liao, Y.-P.; Lin, S.; Meng, H.; Li, R.; Sun, B.; Winkle, L. V.; Pinkerton, K. E.; Zink, J. I.; Xia, T.; Nel, A. E., Use of Coated Silver Nanoparticles to Understand the Relationship of Particle Dissolution and Bioavailability to Cell and Lung Toxicological Potential. *Small* **2014,** *10* (2), 385–398.
47. Badwaik, V. D.; Vangala, L. M.; Pender, D. S.; Willis, C. B.; Aguilar, Z. P.; Gonzalez, M. S.; Paripelly, R.; Dakshinamurthy, R., Size-dependent antimicrobial properties of sugar-encapsulated gold nanoparticles synthesized by a green method. *Nanoscale Research Letters* **2012,** *7*.
48. Wehling, J.; Volkmann, E.; Grieb, T.; Rosenauer, A.; Maas, M.; Treccani, L.; Rezwan, K., A critical study: Assessment of the effect of silica particles from 15 to 500 nm on bacterial viability. *Environmental Pollution* **2013,** *176*, 292–299.
49. Pal, S.; Tak, Y. K.; Song, J. M., Does the antibacterial activity of silver nanoparticles depend on the shape of the nanoparticle? A study of the gram-negative bacterium Escherichia coli. *Applied and Environmental Microbiology* **2007,** *73* (6), 1712–1720.
50. Sadeghi, B.; Garmaroudi, F. S.; Hashemi, M.; Nezhad, H. R.; Nasrollahi, A.; Ardalan, S.; Ardalan, S., Comparison of the anti-bacterial activity on the nanosilver shapes: Nanoparticles, nanorods and nanoplates. *Advanced Powder Technology* **2012,** *23* (1), 22–26.
51. Le Ouay, B.; Stellacci, F., Antibacterial activity of silver nanoparticles: A surface science insight. *Nano Today* **2015,** *10* (3), 339–354.
52. Ashkarran, A. A.; Estakhri, S.; Nezhad, M. R. H.; Eshghi, S., Controlling the Geometry of Silver Nanostructures for Biological Applications. *European Conference on Nano Films – ECNF2012* **2013,** *40*, 76–83.
53. Abramenko, N. B.; Demidova, T. B.; Abkhalimov, E. V.; Ershov, B. G.; Krysanov, E.Y.; Kustov, L. M., Ecotoxicity of different-shaped silver nanoparticles: Case of zebrafish embryos. *Journal of Hazardous Materials* **2018,** *347*, 89–94.
54. Liu, S. B.; Wei, L.; Hao, L.; Fang, N.; Chang, M. W.; Xu, R.; Yang, Y. H.; Chen, Y., Sharper and Faster "Nano Darts" Kill More Bacteria: A Study of Antibacterial Activity of Individually Dispersed Pristine Single-Walled Carbon Nanotube. *ACS Nano* **2009,** *3* (12), 3891–3902.
55. Ansari, M. A.; Khan, H. M.; Khan, A. A.; Ahmad, M. K.; Mahdi, A. A.; Pal, R.; Cameotra, S. S., Interaction of silver nanoparticles with Escherichia coli and their cell envelope biomolecules. *Journal of Basic Microbiology* **2014,** *54* (9), 905–915.
56. Sake, T. M.; Khowessah, O. M.; Motaleb, M. A.; Abd El-Bary, A.; El-Kolaly, M. T.; Swidan, M. M., I-131 doping of silver nanoparticles platform for tumor theranosis guided drug delivery. *European Journal of Pharmaceutical Sciences* **2018,** *122*, 239–245.
57. Liu, W.; Wu, Y. A.; Wang, C.; Li, H. C.; Wang, T.; Liao, C. Y.; Cui, L.; Zhou, Q. F.; Yan, B.; Jiang, G. B., Impact of silver nanoparticles on human cells: Effect of particle size. *Nanotoxicology* **2010,** *4* (3), 319–330.
58. Pan, Y.; Neuss, S.; Leifert, A.; Fischler, M.; Wen, F.; Simon, U.; Schmid, G.; Brandau, W.; Jahnen-Dechent, W., Size-dependent cytotoxicity of gold nanoparticles. *Small* **2007,** *3* (11), 1941–1949.
59. Oberdörster, G.; Maynard, A.; Donaldson, K.; Castranova, V.; Fitzpatrick, J.; Ausman, K.; Carter, J.; Karn, B.; Kreyling, W.; Lai, D.; Olin, S.; Monteiro-Riviere, N.; Warheit, D.; Yang, H.; ILSI Research Foundation/Risk Science Institute Nanomaterial Toxicity Screening Working Group, Principles for characterizing the

potential human health effects from exposure to nanomaterials: elements of a screening strategy. *Particle and fibre toxicology* **2005,** *2* (8).
60. Shang, L.; Nienhaus, K.; Nienhaus, G. U., Engineered nanoparticles interacting with cells: size matters. *Journal of Nanobiotechnology* **2014,** *12*.
61. Qiu, Y.; Liu, Y.; Wang, L.; Xu, L.; Bai, R.; Ji, Y.; Wu, X.; Zhao, Y.; Li, Y.; Chen, C., Surface chemistry and aspect ratio mediated cellular uptake of Au nanorods. *Biomaterials* **2010,** *31* (30), 7606–7619.
62. Graf, C.; Nordmeyer, D.; Sengstock, C.; Ahlberg, S.; Diendorf, J.; Raabe, J.; Epple, M.; Koller, M.; Lademann, J.; Vogt, A.; Rancan, F.; Ruhl, E., Shape-Dependent Dissolution and Cellular Uptake of Silver Nanoparticles. *Langmuir* **2018,** *34* (4), 1506–1519.
63. George, S.; Lin, S.; Jo, Z.; Thomas, C. R.; Li, L.; Mecklenburg, M.; Meng, H.; Wang, X.; Zhang, H.; Xia, T.; Hohman, J. N.; Lin, S.; Zink, J. I.; Weiss, P. S.; Nel, A. E., Surface Defects on Plate-Shaped Silver Nanoparticles Contribute to Its Hazard Potential in a Fish Gill Cell Line and Zebrafish Embryos. *ACS Nano* **2012,** *6* (5), 3745–3759.
64. Stoehr, L. C.; Gonzalez, E.; Stampfl, A.; Casals, E.; Duschl, A.; Puntes, V.; Oostingh, G. J., Shape matters: effects of silver nanospheres and wires on human alveolar epithelial cells. *Particle and Fibre Toxicology* **2011,** *8*.
65. Cho, E. C.; Xie, J.; Wurm, P. A.; Xia, Y., Understanding the Role of Surface Charges in Cellular Adsorption versus Internalization by Selectively Removing Gold Nanoparticles on the Cell Surface with a I2/KI Etchant. *Nano Letters* **2009,** *9* (3), 1080–1084.
66. Choi, S. Y.; Yang, N.; Jeon, S. K.; Yoon, T. H., Semi-quantitative Estimation of Cellular SiO2 Nanoparticles Using Flow Cytometry Combined with X-ray Fluorescence Measurements. *Cytometry Part A* **2014,** *85A* (9), 771–780.
67. Vranic, S.; Boggetto, N.; Contremoulins, V.; Mornet, S.; Reinhardt, N.; Marano, F.; Baeza-Squiban, A.; Boland, S., Deciphering the mechanisms of cellular uptake of engineered nanoparticles by accurate evaluation of internalization using imaging flow cytometry. *Particle and Fibre Toxicology* **2013,** *10*.
68. Harush-Frenkel, O.; Debotton, N.; Benita, S.; Altschuler, Y., Targeting of nanoparticles to the clathrin-mediated endocytic pathway. *Biochemical and Biophysical Research Communications* **2007,** *353* (1), 26–32.
69. Lundqvist, M.; Stigler, J.; Cedervall, T.; Berggard, T.; Flanagan, M. B.; Lynch, I.; Elia, G.; Dawson, K., The Evolution of the Protein Corona around Nanoparticles: A Test Study. *ACS Nano* **2011,** *5* (9), 7503–7509.
70. Walczyk, D.; Bombelli, F. B.; Monopoli, M. P.; Lynch, I.; Dawson, K. A., What the Cell "Sees" in Bionanoscience. *Journal of the American Chemical Society* **2010,** *132* (16), 5761–5768.
71. Wang, L.; Liu, Y.; Li, W.; Jiang, X.; Ji, Y.; Wu, X.; Xu, L.; Qiu, Y.; Zhao, K.; Wei, T.; Li, Y.; Zhao, Y.; Chen, C., Selective Targeting of Gold Nanorods at the Mitochondria of Cancer Cells: Implications for Cancer Therapy. *Nano Letters* **2011,** *11* (2), 772–780.
72. AshaRani, P. V.; Mun, G. L. K.; Hande, M. P.; Valiyaveettil, S., Cytotoxicity and Genotoxicity of Silver Nanoparticles in Human Cells. *ACS Nano* **2009,** *3* (2), 279–290.
73. Ostrowski, A.; Nordmeyer, D.; Boreham, A.; Holzhausen, C.; Mundhenk, L.; Graf, C.; Meinke, M. C.; Vogt, A.; Hadam, S.; Lademann, J.; Ruehl, E.; Alexiev, U.; Gruber, A. D., Overview about the localization of nanoparticles in tissue and cellular

context by different imaging techniques. *Beilstein Journal of Nanotechnology* **2015,** *6*, 263–280.
74. Gibbs-Flournoy, E. A.; Bromberg, P. A.; Hofer, T. P. J.; Samet, J. M.; Zucker, R. M., Darkfield-Confocal Microscopy detection of nanoscale particle internalization by human lung cells. *Particle and Fibre Toxicology* **2011,** *8*.
75. Müller, T.; Schumann, C.; Kraegeloh, A., STED Microscopy and its Applications: New Insights into Cellular Processes on the Nanoscale. *ChemPhysChem* **2012,** *13* (8), 1986–2000.
76. Uchiyama, M. K.; Deda, D. K.; de Paula Rodrigues, S. F.; Drewes, C. C.; Bolonheis, S. M.; Kiyohara, P. K.; de Toledo, S. P.; Colli, W.; Araki, K.; Poliselli Farsky, S. H., In vivo and In vitro Toxicity and Anti-Inflammatory Properties of Gold Nanoparticle Bioconjugates to the Vascular System. *Toxicological Sciences* **2014,** *142* (2), 497–507.
77. Suzuki, H.; Toyooka, T.; Ibuki, Y., Simple and easy method to evaluate uptake potential of nanoparticles in mammalian cells using a flow cytometric light scatter analysis. *Environmental Science & Technology* **2007,** *41* (8), 3018–3024.
78. Zucker, R. M.; Daniel, K. M.; Massaro, E. J.; Karafas, S. J.; Degn, L. L.; Boyes, W. K., Detection of Silver Nanoparticles in Cells by Flow Cytometry Using Light Scatter and Far-Red Fluorescence. *Cytometry Part A* **2013,** *83* (10), 962–972.
79. Zucker, R. M.; Daniel, K. M., Detection of TiO2 nanoparticles in cells by flow cytometry. *Cytometry Part A* **2010,** *77A* (7), 677–685.
80. Boehme, S.; Staerk, H.-J.; Meissner, T.; Springer, A.; Reemtsma, T.; Kuehnel, D.; Busch, W., Quantification of Al2O3 nanoparticles in human cell lines applying inductively coupled plasma mass spectrometry (neb-ICP-MS, LA-ICP-MS) and flow cytometry-based methods. *Journal of Nanoparticle Research* **2014,** *16* (9).
81. Braun, G. B.; Friman, T.; Pang, H.-B.; Pallaoro, A.; de Mendoza, T. H.; Willmore, A.-M. A.; Kotamraju, V. R.; Mann, A. P.; She, Z.-G.; Sugahara, K. N.; Reich, N. O.; Teesalu, T.; Ruoslahti, E., Etchable plasmonic nanoparticle probes to image and quantify cellular internalization. *Nature Materials* **2014,** *13* (9), 904–911.
82. Project on Emerging Nanotechnologies (2013). Consumer Products Inventory. Retrieved September 24th 2018, from http://www.nanotechproject.org/cpi.
83. The Nanodatabase. Retrieved September 24th 2018, from http://nanodb.dk/.
84. Moritz, M.; Geszke-Moritz, M., The newest achievements in synthesis, immobilization and practical applications of antibacterial nanoparticles. *Chemical Engineering Journal* **2013,** *228*, 596–613.
85. Helmlinger, J.; Sengstock, C.; Gross-Heitfeld, C.; Mayer, C.; Schildhauer, T. A.; Koeller, M.; Epple, M., Silver nanoparticles with different size and shape: equal cytotoxicity, but different antibacterial effects. *RSC Advances* **2016,** *6* (22), 18490–18501.
86. Silver, S., Bacterial silver resistance: molecular biology and uses and misuses of silver compounds. *FEMS Microbiology Reviews* **2003,** *27* (2–3), 341–353.
87. Klein, E. Y.; Van Boeckel, T. P.; Martinez, E. M.; Pant, S.; Gandra, S.; Levin, S. A.; Goossens, H.; Laxminarayan, R., Global increase and geographic convergence in antibiotic consumption between 2000 and 2015. *Proceedings of the National Academy of Sciences of the United States of America* **2018,** *115* (15), E3463–E3470.
88. Franci, G.; Falanga, A.; Galdiero, S.; Palomba, L.; Rai, M.; Morelli, G.; Galdiero, M., Silver Nanoparticles as Potential Antibacterial Agents. *Molecules* **2015,** *20* (5), 8856–8874.

89. Page, K.; Wilson, M.; Parkin, I. P., Antimicrobial surfaces and their potential in reducing the role of the inanimate environment in the incidence of hospital-acquired infections. *Journal of Materials Chemistry* **2009,** *19* (23), 3819–3831.
90. Green, J-B. D.; Fulghum, T.; Nordhaus, M.A., Immobilized Antimicrobial Agents: A Critical Perspective. *Science Against Microbial Pathogens: Communicating Current Research and Technological Advances*, **2011**, 1: 84–98.
91. Pogodin, S.; Hasan, J.; Baulin, V. A.; Webb, H. K.; Vi Khanh, T.; The Hong Phong, N.; Boshkovikj, V.; Fluke, C. J.; Watson, G. S.; Watson, J. A.; Crawford, R. J.; Ivanova, E. P., Biophysical Model of Bacterial Cell Interactions with Nanopatterned Cicada Wing Surfaces. *Biophysical Journal* **2013,** *104* (4), 835–840.
92. Yuan, Y.; Zhang, Y., Enhanced biomimic bactericidal surfaces by coating with positively-charged ZIF nano-dagger arrays. *Nanomedicine: Nanotechnology, Biology and Medicine* **2017,** *13* (7), 2199–2207.
93. Gottenbos, B.; Grijpma, D. W.; van der Mei, H. C.; Feijen, J.; Busscher, H. J., Antimicrobial effects of positively charged surfaces on adhering Gram-positive and Gram-negative bacteria. *Journal of Antimicrobial Chemotherapy* **2001,** *48* (1), 7–13.
94. Hasan, J.; Crawford, R. J.; Lvanova, E. P., Antibacterial surfaces: the quest for a new generation of biomaterials. *Trends in Biotechnology* **2013,** *31* (5), 31–40.
95. Grass, G.; Rensing, C.; Solioz, M., Metallic Copper as an Antimicrobial Surface. *Applied and Environmental Microbiology* **2011,** *77* (5), 1541–1547.
96. Lemire, J. A.; Harrison, J. J.; Turner, R. J., Antimicrobial activity of metals: mechanisms, molecular targets and applications. *Nature Reviews Microbiology* **2013,** *11* (6), 371–384.
97. Villapun, V. M.; Dover, L. G.; Cross, A.; Gonzalez, S., Antibacterial Metallic Touch Surfaces. *Materials* **2016,** *9* (9).
98. Vimbela, G. V.; Ngo, S. M.; Fraze, C.; Yang, L.; Stout, D. A., Antibacterial properties and toxicity from metallic nanomaterials. *International Journal of Nanomedicine* **2017,** *12*, 3941–3965.
99. Ahonen, M.; Kahru, A.; Ivask, A.; Kasemets, K.; Kõljalg, S.; Mantecca, P.; Vrcek, I. V.; Keinanen-Toivola, M. M.; Crijns, F., Proactive Approach for Safe Use of Antimicrobial Coatings in Healthcare Settings: Opinion of the COST Action Network AMiCI. *International Journal of Environmental Research and Public Health* **2017,** *14* (4).
100. Foster, H. A.; Ditta, I. B.; Varghese, S.; Steele, A., Photocatalytic disinfection using titanium dioxide: spectrum and mechanism of antimicrobial activity. *Applied Microbiology and Biotechnology* **2011,** *90* (6), 1847–1868.
101. Kubacka, A.; Diez, M. S.; Rojo, D.; Bargiela, R.; Ciordia, S.; Zapico, I.; Albar, J. P.; Barbas, C.; dos Santos, V.; Fernandez-Garcia, M.; Ferrer, M., Understanding the antimicrobial mechanism of TiO2-based nanocomposite films in a pathogenic bacterium. *Scientific Reports* **2014,** *4*.
102. Sirelkhatim, A.; Mahmud, S.; Seeni, A.; Kaus, N. H. M.; Ann, L. C.; Bakhori, S. K. M.; Hasan, H.; Mohamad, D., Review on Zinc Oxide Nanoparticles: Antibacterial Activity and Toxicity Mechanism. *Nano-Micro Letters* **2015,** *7* (3), 219–242.
103. Kahru, A.; Dubourguier, H.-C., From ecotoxicology to nanoecotoxicology. *Toxicology* **2010,** *269* (2–3), 105–119.
104. Keshmiri, M.; Mohseni, M.; Troczynski, T., Development of novel TiO2 sol-gel-derived composite and its photocatalytic activities for trichloroethylene oxidation. *Applied Catalysis B: Environmental* **2004,** *53* (4), 209–219.

105. Kiema, G. K.; Colgan, M. J.; Brett, M. J., Dye sensitized solar cells incorporating obliquely deposited titanium oxide layers. *Solar Energy Materials and Solar Cells* **2005,** *85* (3), 321–331.
106. Wang, R.; Hashimoto, K.; Fujishima, A.; Chikuni, M.; Kojima, E.; Kitamura, A.; Shimohigoshi, M.; Watanabe, T., Light-induced amphiphilic surfaces. *Nature* **1997,** *388* (6641), 431–432.
107. Wang, R.; Hashimoto, K.; Fujishima, A.; Chikuni, M.; Kojima, E.; Kitamura, A.; Shimohigoshi, M.; Watanabe, T., Photogeneration of highly amphiphilic TiO2 surfaces. *Advanced Materials* **1998,** *10* (2), 135–+.
108. Kiwi, J.; Nadtochenko, V., New evidence for TiO2 photocatalysis during bilayer lipid peroxidation. *Journal of Physical Chemistry B* **2004,** *108* (45), 17675–17684.
109. Rizzo, L.; Della Sala, A.; Fiorentino, A.; Puma, G. L., Disinfection of urban wastewater by solar driven and UV lamp – TiO2 photocatalysis: Effect on a multi drug resistant Escherichia coli strain. *Water Research* **2014,** *53*, 145–152.
110. Carp, O.; Huisman, C. L.; Reller, A., Photoinduced reactivity of titanium dioxide. *Progress in Solid State Chemistry* **2004,** *32* (1–2), 33–177.
111. Lee, N. C.; Choi, W. Y., Solid phase photocatalytic reaction on the soot/TiO2 interface: The role of migrating OH radicals. *Journal of Physical Chemistry B* **2002,** *106* (45), 11818–11822.
112. Kuhn, K. P.; Chaberny, I. F.; Massholder, K.; Stickler, M.; Benz, V. W.; Sonntag, H. G.; Erdinger, L., Disinfection of surfaces by photocatalytic oxidation with titanium dioxide and UVA light. *Chemosphere* **2003,** *53* (1), 71–77.
113. Ong, C. B.; Ng, L. Y.; Mohammad, A. W., A review of ZnO nanoparticles as solar photocatalysts: Synthesis, mechanisms and applications. *Renewable & Sustainable Energy Reviews* **2018,** *81*, 536–551.
114. Kumar, R.; Umar, A.; Kumar, G.; Nalwa, H. S., Antimicrobial properties of ZnO nanomaterials: A review. *Ceramics International* **2017,** *43* (5), 3940–3961.
115. Georgekutty, R.; Seery, M. K.; Pillai, S. C., A highly efficient Ag-ZnO photocatalyst: Synthesis, properties, and mechanism. *Journal of Physical Chemistry C* **2008,** *112* (35), 13563–13570.
116. Lu, W.; Liu, G.; Gao, S.; Xing, S.; Wang, J., Tyrosine-assisted preparation of Ag/ZnO nanocomposites with enhanced photocatalytic performance and synergistic antibacterial activities. *Nanotechnology* **2008,** *19* (44).
117. Thomas, M. A.; Cui, J. B., Electrochemical Route to p-Type Doping of ZnO Nanowires. *Journal of Physical Chemistry Letters* **2010,** *1* (7), 1090–1094.
118. Thongsuriwong, K.; Amornpitoksuk, P.; Suwanboon, S., Photocatalytic and antibacterial activities of Ag-doped ZnO thin films prepared by a sol-gel dip-coating method. *Journal of Sol-Gel Science and Technology* **2012,** *62* (3), 304–312.
119. Talari, M. K.; Majeed, A. B. A.; Tripathi, D. K.; Tripathy, M., Synthesis, Characterization and Antimicrobial Investigation of Mechanochemically Processed Silver Doped ZnO Nanoparticles. *Chemical & Pharmaceutical Bulletin* **2012,** *60* (7), 818–824.
120. Chen, Y.; Tse, W. H.; Chen, L.; Zhang, J., Ag nanoparticles-decorated ZnO nanorod array on a mechanical flexible substrate with enhanced optical and antimicrobial properties. *Nanoscale Research Letters* **2015,** *10*.
121. Ekthammathat, N.; Thongtem, S.; Thongtem, T.; Phuruangrat, A., Characterization and antibacterial activity of nanostructured ZnO thin films synthesized through a hydrothermal method. *Powder Technology* **2014,** *254*, 199–205.

122. Torrey, J. D.; Kirschling, T. L.; Greenlee, L. F., Processing and Characterization of Nanoparticle Coatings for Quartz Crystal Microbalance Measurements. *Journal of Research of the National Institute of Standards and Technology* **2015,** *120*, 1–10.
123. Ghorbani, H. R.; Safekordi, A. A.; Attar, H.; Sorkhabadi, S. M. R., Biological and Non-biological Methods for Silver Nanoparticles Synthesis. *Chemical and Biochemical Engineering Quarterly* **2011,** *25* (3), 317–326.
124. Rivas, L.; Sanchez-Cortes, S.; Garcia-Ramos, J. V.; Morcillo, G., Growth of silver colloidal particles obtained by citrate reduction to increase the Raman enhancement factor. *Langmuir* **2001,** *17* (3), 574–577.
125. Tzeng, S. K.; Hon, M. H.; Leu, I. C., Improving the Performance of a Zinc Oxide Nanowire Ultraviolet Photodetector by Adding Silver Nanoparticles. *Journal of the Electrochemical Society* **2012,** *159* (4), H440–H443.
126. Ren, C.; Yang, B.; Wu, M.; Xu, J.; Fu, Z.; Lv, Y.; Guo, T.; Zhao, Y.; Zhu, C., Synthesis of Ag/ZnO nanorods array with enhanced photocatalytic performance. *Journal of Hazardous Materials* **2010,** *182* (1–3), 123–129.
127. Rigo, S.; Cai, C.; Gunkel-Grabole, G.; Maurizi, L.; Zhang, X.; Xu, J.; Palivan, C. G., Nanoscience-Based Strategies to Engineer Antimicrobial Surfaces. *Advanced Science* **2018,** *5* (5).
128. Green, J-B. D.; Fulghum, T.; Nordhaus, M.A., A review of immobilized antimicrobial agents and methods for testing. *Biointerphases* **2011,** *6* (4), MR13–MR28.
129. International Organization for Standardization, ISO 27447:2009 Fine ceramics (advanced ceramics, advanced technical ceramics)-Test method for antibacterial activity of semiconducting photocatalytic materials. 2009.
130. Marambio-Jones, C.; Hoek, E. M. V., A review of the antibacterial effects of silver nanomaterials and potential implications for human health and the environment. *Journal of Nanoparticle Research* **2010,** *12* (5), 1531–1551.
131. Stensberg, M. C.; Wei, Q.; McLamore, E. S.; Porterfield, D. M.; Wei, A.; Sepulveda, M. S., Toxicological studies on silver nanoparticles: challenges and opportunities in assessment, monitoring and imaging. *Nanomedicine* **2011,** *6* (5), 879–898.
132. Zhao, G. J.; Stevens, S. E., Multiple parameters for the comprehensive evaluation of the susceptibility of Escherichia coli to the silver ion. *Biometals* **1998,** *11* (1), 27–32.
133. Ivask, A.; Rõlova, T.; Kahru, A., A suite of recombinant luminescent bacterial strains for the quantification of bioavailable heavy metals and toxicity testing. *BMC Biotechnology* **2009,** *9*.
134. Kurvet, I.; Ivask, A.; Bondarenko, O.; Sihtmäe, M.; Kahru, A., LuxCDABE-Transformed Constitutively Bioluminescent Escherichia coli for Toxicity Screening: Comparison with Naturally Luminous Vibrio fischeri. *Sensors* **2011,** *11* (8), 7865–7878.
135. Thorn, R. M. S.; Nelson, S. M.; Greenman, J., Use of a bioluminescent Pseudomonas aeruginosa strain within an in vitro microbiological system, as a model of wound infection, to assess the antimicrobial efficacy of wound dressings by monitoring light production. *Antimicrobial Agents and Chemotherapy* **2007,** *51* (9), 3217–3224.
136. Ma, R.; Levard, C.; Marinakos, S. M.; Cheng, Y.; Liu, J.; Michel, F. M.; Brown, G. E., Jr.; Lowry, G. V., Size-Controlled Dissolution of Organic-Coated Silver Nanoparticles. *Environmental Science & Technology* **2012,** *46* (2), 752–759.

137. Wang, L.; Zhang, T.; Li, P.; Huang, W.; Tang, J.; Wang, P.; Liu, J.; Yuan, Q.; Bai, R.; Li, B.; Zhang, K.; Zhao, Y.; Chen, C., Use of Synchrotron Radiation-Analytical Techniques To Reveal Chemical Origin of Silver-Nanoparticle Cytotoxicity. *ACS Nano* **2015,** *9* (6), 6532–6547.
138. Kudish, A. I.; Lyubansky, V.; Evseev, E. G.; Ianetz, A., Inter-comparison of the solar UVB, UVA and global radiation clearness and UV indices for Beer Sheva and Neve Zohar (Dead Sea), Israel. *Energy* **2005,** *30* (9), 1623–1641.
139. Wang, R. M.; Wang, B. Y.; He, Y. F.; Lv, W. H.; Wang, J. F., Preparation of composited Nano-TiO2 and its application on antimicrobial and self-cleaning coatings. *Polymers for Advanced Technologies* **2010,** *21* (5), 331–336.
140. Shiraishi, K.; Koseki, H.; Tsurumoto, T.; Baba, K.; Naito, M.; Nakayama, K.; Shindo, H., Antibacterial metal implant with a TiO(2)-conferred photocatalytic bactericidal effect against Staphylococcus aureus. *Surface and Interface Analysis* **2009,** *41* (1), 17–22.
141. Day, A. P.; Oliver, J. D., Changes in membrane fatty acid composition during entry of Vibrio vulnificus into the viable but nonculturable state. *Journal of Microbiology* **2004,** *42* (2), 69–73.
142. Or-Rashid, M. M.; Odongo, N. E.; McBride, B. W., Fatty acid composition of ruminal bacteria and protozoa, with emphasis on conjugated linoleic acid, vaccenic acid, and odd-chain and branched-chain fatty acids. *Journal of Animal Science* **2007,** *85* (5), 1228–1234.
143. Schumann, J.; Leichtle, A.; Thiery, J.; Fuhrmann, H., Fatty Acid and Peptide Profiles in Plasma Membrane and Membrane Rafts of PUFA Supplemented RAW264.7 Macrophages. *PLOS ONE* **2011,** *6* (8).
144. Leung, T. Y.; Chan, C. Y.; Hu, C.; Yu, J. C.; Wong, P. K., Photocatalytic disinfection of marine bacteria using fluorescent light. *Water Research* **2008,** *42* (19), 4827–4837.
145. Zheng, Y.; Zheng, L.; Zhan, Y.; Lin, X.; Zheng, Q.; Wei, K., Ag/ZnO heterostructure nanocrystals: Synthesis, characterization, and photocatalysis. *Inorganic Chemistry* **2007,** *46* (17), 6980–6986.
146. Bechambi, O.; Chalbi, M.; Najjar, W.; Sayadi, S., Photocatalytic activity of ZnO doped with Ag on the degradation of endocrine disrupting under UV irradiation and the investigation of its antibacterial activity. *Applied Surface Science* **2015,** *347*, 414–420.
147. Pyne, S.; Sahoo, G. P.; Bhui, D. K.; Bar, H.; Sarkar, P.; Samanta, S.; Maity, A.; Misra, A., Enhanced photocatalytic activity of metal coated ZnO nanowires. *Spectrochimica Acta Part A: Molecular and Biomolecular Spectroscopy* **2012,** *93*, 100–105.
148. Sun, F.; Tan, F.; Wang, W.; Qiao, X.; Qiu, X., Facile synthesis of Ag/ZnO heterostructure nanocrystals with enhanced photocatalytic performance. *Materials Research Bulletin* **2012,** *47* (11), 3357–3361.
149. Deng, Q.; Duan, X.; Ng, D. H. L.; Tang, H.; Yang, Y.; Kong, M.; Wu, Z.; Cai, W.; Wang, G., Ag Nanoparticle Decorated Nanoporous ZnO Microrods and Their Enhanced Photocatalytic Activities. *ACS Applied Materials & Interfaces* **2012,** *4* (11), 6030–6037.
150. Meng, A.; Xing, J.; Li, Z.; Wei, Q.; Li, Q., Ag/AgCl/ZnO nano-networks: Preparation, characterization, mechanism and photocatalytic activity. *Journal of Molecular Catalysis A: Chemical* **2016,** *411*, 290–298.

151. Evanoff, D. D.; Chumanov, G., Synthesis and optical properties of silver nanoparticles and arrays. *ChemPhysChem* **2005,** *6* (7), 1221–1231.
152. Zeelie, J. J.; McCarthy, T. J., Effects of copper and zinc ions on the germicidal properties of two popular pharmaceutical antiseptic agents cetylpyridinium chloride and povidone-iodine. *Analyst* **1998,** *123* (3), 503–507.
153. Applerot, G.; Lipovsky, A.; Dror, R.; Perkas, N.; Nitzan, Y.; Lubart, R.; Gedanken, A., Enhanced Antibacterial Activity of Nanocrystalline ZnO Due to Increased ROS-Mediated Cell Injury. *Advanced Functional Materials* **2009,** *19* (6), 842–852.
154. Al-Jawad, S. M. H.; Sabeeh, S. H.; Taha, A. A.; Jassim, H. A., Studying structural, morphological and optical properties of nanocrystalline ZnO:Ag films prepared by sol-gel method for antimicrobial activity. *Journal of Sol-Gel Science and Technology* **2018,** *87* (2), 362–371.
155. Pan, X.; Peng, L.; Liu, Y.; Wang, J., Highly Antibacterial and Toughened Polystyrene Composites with Silver Nanoparticles Modified Tetrapod-Like Zinc Oxide Whiskers. *Journal of Applied Polymer Science* **2014,** *131* (20).
156. Hirota, K.; Sugimoto, M.; Kato, M.; Tsukagoshi, K.; Tanigawa, T.; Sugimoto, H., Preparation of zinc oxide ceramics with a sustainable antibacterial activity under dark conditions. *Ceramics International* **2010,** *36* (2), 497–506.
157. Prasanna, V. L.; Vijayaraghavan, R., Insight into the Mechanism of Antibacterial Activity of ZnO: Surface Defects Mediated Reactive Oxygen Species Even in the Dark. *Langmuir* **2015,** *31* (33), 9155–9162.
158. Manna, J.; Goswami, S.; Shilpa, N.; Sahu, N.; Rana, R. K., Biomimetic Method To Assemble Nanostructured Ag@ZnO on Cotton Fabrics: Application as Self-Cleaning Flexible Materials with Visible-Light Photocatalysis and Antibacterial Activities. *ACS Applied Materials & Interfaces* **2015,** *7* (15), 8076–8082.
159. Joe, A.; Park, S.-H.; Shim, K.-D.; Kim, D.-J.; Jhee, K.-H.; Lee, H.-W.; Heo, C.-H.; Kim, H.-M.; Jang, E.-S., Antibacterial mechanism of ZnO nanoparticles under dark conditions. *Journal of Industrial and Engineering Chemistry* **2017,** *45*, 430–439.

ACKNOWLEDGEMENTS

First and foremost, I'm very grateful to my supervisors Dr. Vambola Kisand and Dr. Angela Ivask for their tireless support, guidance and encouragement during my PhD studies. We have had an eventful and enriching journey together. I'm very grateful to my supervisor Dr. Margit Heinlaan for her suggestions and constructive attitude.

This study was carried out in collaboration with the National Institute of Chemical Physics and Biophysics and I would like to thank Dr. Anne Kahru, the head of the Laboratory of Environmental Toxicology, for welcoming me to her research group and for enabling a friendly and encouraging working environment.

I'm thankful to all my colleagues and co-authors with whom it`s been a pleasure to work with. I would like to thank Rando Saar and Dr. Mihkel Rähn for their help with SEM/EDX and TEM measurements. My special thanks go to Katre and Merilin for supporting me in the world of microbes and to Urmas for always having answers to my endless questions. The "(Ex-)PhD student get-togethers" have been a priceless bonus to the collaboration with the Laboratory of Environmental Toxicology. I appreciate the group of Imaginaarkuivikud with whom I've shared memorable moments and great laughs (in between scientific discussions, of course).

Finally, I thank my parents and my two brothers for their lifelong support and unquestionable belief in all my decisions. I thank you, Liis and Sille for being an invaluable part of my life and for keeping up my motivation when needed.

This work was financially supported by the following agencies and foundations: Estonian Research Council (Grants ETF8216, PUT748, IUT2-25 and IUT23-5), EU FP7 NanoValid Project (Contract 263147), ERF project Graduate School of Functional Materials and Technologies, European Social Fund's Doctoral Studies and Internationalisation Programme DoRa, Estonian Centre of Excellence in Research Projects "Emerging orders in quantum and nanomaterials (TK134)", "Advanced materials and high-technology devices for sustainable energetics, sensorics and nanoelectronics (TK141)", "High-technology Materials for Sustainable Development" (TK117), "Mesosystems – Theory and Applications" (TK114).

PUBLICATIONS

CURRICULUM VITAE

Name: Meeri Visnapuu
Date of birth: 10.02.1988
Nationality: Estonian
E-mail: meeri.visnapuu@ut.ee

Education:

2011–…	University of Tartu, Faculty of Science and Technology, PhD student of Engineering and Technology
2009–2011	University of Tartu, Faculty of Science and Technology, Master of Science in Engineering (Materials Science), *cum laude*
2006–2009	University of Tartu, Faculty of Science and Technology, Bachelor of Science in Engineering (Materials Science)
1995–2006	Kadrina Secondary School, silver medal
1994–1995	Vohnja Kindergarten-Primary School

Career:

2019–…	University of Tartu, Institute of Physics, specialist
2015–2018	National Institute of Chemical Physics and Biophysics, Early-Stage Researcher
2012–2014	University of Tartu, Institute of Physics, specialist
2010–2012	University of Tartu, Institute of Technology, laboratory technician
2008–2010	University of Tartu, Institute of Physics, laboratory technician

Special courses:

2015	Archimedes Foundation DoRa T6 scholarship: semester abroad for Doctoral students (Adelaide, Australia, University of South Australia)
2014	"Practical Course in Advanced Microscopy" (Zürich, Switzerland, ETH Zürich and University of Zürich) "Modern morphological methods" (Tartu, Estonia, Estonian University of Life Sciences)
2013	"Implications of Nanomaterials: A hands on course on Synthesis, Characterisation, and Ecotoxicology" (Aveiro, Portugal, University of Aveiro)

Supervised dissertations:

1. Egle Truska, Master's Degree, 2018, supervisors Merilin Rosenberg, Meeri Visnapuu; Optimization of antimicrobial and photocatalytic properties of nano-ZnO/Ag composite covered surfaces, Tallinn University of Technology.

2. Adam Erki Enok, Master's Degree, 2016, supervisors Urmas Joost, Meeri Visnapuu, Vambola Kisand; Optically transparent aluminium doped zinc oxide thin films from alkyl amine stabilised nano dispersions – preparation and characterisation, University of Tartu.
3. Meeri Lembinen, Master's Degree, 2014, supervisors Vambola Kisand, Urmas Joost, Meeri Visnapuu; Spectral dependence of the orientation and the size of metallic nanorods, University of Tartu.

List of publications:

1. A. Šutka, M. Järvekülg, K. A. Gross, M. Kook, T. Käämbre, **M. Visnapuu**, G. Trefalt, A. Šutka, Visible light to switch-on desorption from goethite, *Nanoscale* 11 (2019) 3794–3798.
2. **M. Visnapuu**, M. Rosenberg, E. Truska, E. Nõmmiste, A. Šutka, A. Kahru, M. Rähn, H. Vija, K. Orupõld, V. Kisand, A. Ivask, UVA-induced antimicrobial activity of ZnO/Ag nano-composite covered surfaces, *Colloids and Surfaces B: Biointerfaces* 169 (2018) 222–232.
3. A. Ivask, E. H. Pilkington, T. Blin, A. Käkinen, H. Vija, **M. Visnapuu**, J. F. Quinn, M. R. Whittaker, R. Qiao, T. P. Davis, P.-C. Ke, N. H. Voelcker, Uptake and transcytosis of functionalized superparamagnetic iron oxide nanoparticles in an in vitro blood brain barrier model, *Biomaterials Science* 6 (2018) 314–323.
4. A. Šutka, M. Antsov, M. Järvekülg, **M. Visnapuu**, I. Heinmaa, U. Mäeorg, S. Vlassov, A. Šutka, Mechanical properties of individual fiber segments of electrospun lignocellulose-reinforced poly(vinyl alcohol), *Journal of Applied Polymer Science* 134 (2017) 44361.
5. U. Joost, A. Šutka, **M. Visnapuu**, A. Tamm, M. Lembinen, M. Antsov, K. Utt, K. Smits, E. Nõmmiste, V. Kisand, Colorimetric gas detection by the varying thickness of a thin film of ultrasmall PTSA-coated TiO_2 nanoparticles on a Si substrate, *Beilstein Journal of Nanotechnology* 8 (2017) 229−236.
6. A. Ivask, **M. Visnapuu**, P. Vallotton, E. R. Marzouk, E. Lombi, N. H. Voelcker, Quantitative multimodal analyses of silver nanoparticle-cell interactions: Implications for cytotoxicity, *NanoImpact* 1 (2016) 29–38.
7. U. Joost, K. Juganson, **M. Visnapuu**, M. Mortimer, A. Kahru, E. Nõmmiste, U. Joost, V. Kisand, A. Ivask, Photocatalytic antibacterial activity of nano-TiO_2 (anatase)-based thin films: Effects on *Escherichia coli* cells and fatty acids, *Journal of Photochemistry and Photobiology B: Biology* 142 (2015) 178–185.
8. O. M. Bondarenko, A. Ivask, A. Kahru, H. Vija, T. Titma, **M. Visnapuu**, U. Joost, K. Pudova, S. Adamberg, T. Visnapuu, T. Alamäe, Bacterial polysaccharide levan as stabilizing, non-toxic and functional coating material for microelement-nanoparticles, *Carbohydrate Polymers* 136 (2015) 710−720.

9. A. Šutka, M. Timusk, N. Döbelin, R. Pärna, **M. Visnapuu**, U. Joost, T. Käämbre, V. Kisand, K. Saal, M. Knite, A straightforward and "green" solvothermal synthesis of Al doped zinc oxide plasmonic nanocrystals and piezoresistive elastomer nanocomposite, *RSC Advances* 5 (2015) 63846−63852.
10. A. Ivask, T. Titma, **M. Visnapuu**, H. Vija, A. Käkinen, M. Sihtmäe, S. Pokhel, L. Madler, M. Heinlaan, V. Kisand, R. Shimmo, A. Kahru, Toxicity of 11 Metal Oxide Nanoparticles to Three Mammalian Cell Types In Vitro, *Current Topics in Medicinal Chemistry* 15 (2015), 1914−1929.
11. A. Ivask, I. Kurvet, K. Kasemets, I. Blinova, V. Aruoja, S. Suppi, H. Vija, A. Käkinen, T. Titma, M. Heinlaan, **M. Visnapuu**, D. Koller, V. Kisand, A. Kahru, Size-dependent Toxicity of Silver Nanoparticles to Bacteria, Yeast, Algae, Crustaceans and Mammalian Cells in Vitro, *PLOS ONE* 9 (2014) e102108.
12. U. Joost, A. Saarva, **M. Visnapuu**, E. Nõmmiste, K. Utt, R. Saar, V. Kisand, Purification of titania nanoparticle thin films: Triviality or a challenge? *Ceramics International* 40 (2014), 7125−7132.
13. **M. Visnapuu**, U. Joost, K. Juganson, K. Künnis-Beres, A. Kahru, V. Kisand, A. Ivask, Dissolution of silver nanowires and nanospheres dictates their toxicity to *Escherichia coli*, *BioMed Research International* (2013) 819252.
14. U. Joost, R. Pärna, M. Lembinen, K. Utt, I. Kink, **M. Visnapuu**, V. Kisand, Heat treatment and substrate dependent properties of titania thin films with high copper loading, *Physica Status Solidi A – Applications and Materials Science* 210 (2013) 1201–1212.

ELULOOKIRJELDUS

Nimi: Meeri Visnapuu
Sünniaeg: 10.02.1988
Kodakondsus: Eesti
E-post: meeri.visnapuu@ut.ee

Hariduskäik:

2011–…	Tartu Ülikool, Loodus- ja täppisteaduste valdkond, tehnika ja tehnoloogia doktorant
2009–2011	Tartu Ülikool, Tehnikateaduse magister (materjaliteadus), *cum laude*
2006–2009	Tartu Ülikool, Tehnikateaduse bakalaureus (materjaliteadus)
1995–2006	Kadrina Keskkool, hõbemedal
1994–1995	Vohnja Lasteaed-Algkool

Teenistuskäik:

2019–…	Tartu Ülikooli Füüsika Instituut, spetsialist
2015–2018	Keemilise ja Bioloogilise Füüsika Instituut, nooremteadur
2012–2014	Tartu Ülikooli Füüsika Instituut, spetsialist
2010–2012	Tartu Ülikooli Tehnoloogiainstituut, laborant
2008–2010	Tartu Ülikooli Füüsika Instituut, laborant

Täiendkoolitused:

2015	SA Archimedes DoRa T6 stipendium: doktorantide semester välismaal (Adelaide, Austraalia, Lõuna-Austraalia Ülikool)
2014	mikroskoopia kursus edasijõudnutele "Practical Course in Advanced Microscopy" (Zürich, Šveits, ETH Zürich ja Zürichi ülikool)
	kursus "Kaasaegsed morfoloogia meetodid" (Tartu, Eesti, Eesti Maaülikool)
2013	kursus nanoosakeste sünteesi, iseloomustamise ja ökotoksilisuse kohta "Implications of Nanomaterials: A hands on course on Synthesis, Characterisation, and Ecotoxicology" (Aveiro, Portugal, Aveiro Ülikool)

Juhendatud lõputööd:

1. Egle Truska, magistrikraad, 2018, juhendajad Merilin Rosenberg, Meeri Visnapuu; Nano-ZnO/Ag komposiitsete osakestega kaetud pindade antimikroobsete ja fotokatalüütiliste omaduste optimeerimine, Tallinna Tehnikaülikool.
2. Adam Erki Enok, magistrikraad, 2016, juhendajad Urmas Joost, Meeri Visnapuu, Vambola Kisand; Alküülamiinidega stabiliseeritud alumiiniumiga dopeeritud tsinkoksiidi nanoosakestest optiliselt läbipaistvate kilede valmistamine ja karakteriseerimine, Tartu Ülikool.

3. Meeri Lembinen, magistrikraad, 2014, juhendajad Vambola Kisand, Urmas Joost, Meeri Visnapuu; Metalliliste nanovarraste spektraalomaduste sõltuvus orientatsioonist ja mõõtmetest, Tartu Ülikool.

Publikatsioonide loetelu:

1. A. Šutka, M. Järvekülg, K. A. Gross, M. Kook, T. Käämbre, **M. Visnapuu**, G. Trefalt, A. Šutka, Visible light to switch-on desorption from goethite, *Nanoscale* 11 (2019) 3794–3798.
2. **M. Visnapuu**, M. Rosenberg, E. Truska, E. Nõmmiste, A. Šutka, A. Kahru, M. Rähn, H. Vija, K. Orupõld, V. Kisand, A. Ivask, UVA-induced antimicrobial activity of ZnO/Ag nano-composite covered surfaces, *Colloids and Surfaces B: Biointerfaces* 169 (2018) 222–232.
3. A. Ivask, E. H. Pilkington, T. Blin, A. Käkinen, H. Vija, **M. Visnapuu**, J. F. Quinn, M. R. Whittaker, R. Qiao, T. P. Davis, P.-C. Ke, N. H. Voelcker, Uptake and transcytosis of functionalized superparamagnetic iron oxide nanoparticles in an in vitro blood brain barrier model, *Biomaterials Science* 6 (2018) 314–323.
4. A. Šutka, M. Antsov, M. Järvekülg, **M. Visnapuu**, I. Heinmaa, U. Mäeorg, S. Vlassov, A. Šutka, Mechanical properties of individual fiber segments of electrospun lignocellulose-reinforced poly(vinyl alcohol), *Journal of Applied Polymer Science* 134 (2017) 44361.
5. U. Joost, A. Šutka, **M. Visnapuu**, A. Tamm, M. Lembinen, M. Antsov, K. Utt, K. Smits, E. Nõmmiste, V. Kisand, Colorimetric gas detection by the varying thickness of a thin film of ultrasmall PTSA-coated TiO_2 nanoparticles on a Si substrate, *Beilstein Journal of Nanotechnology* 8 (2017) 229−236.
6. A. Ivask, **M. Visnapuu**, P. Vallotton, E. R. Marzouk, E. Lombi, N. H. Voelcker, Quantitative multimodal analyses of silver nanoparticle-cell interactions: Implications for cytotoxicity, *NanoImpact* 1 (2016) 29–38.
7. U. Joost, K. Juganson, **M. Visnapuu**, M. Mortimer, A. Kahru, E. Nõmmiste, U. Joost, V. Kisand, A. Ivask, Photocatalytic antibacterial activity of nano-TiO_2 (anatase)-based thin films: Effects on *Escherichia coli* cells and fatty acids, *Journal of Photochemistry and Photobiology B: Biology* 142 (2015) 178–185.
8. O. M. Bondarenko, A. Ivask, A. Kahru, H. Vija, T. Titma, **M. Visnapuu**, U. Joost, K. Pudova, S. Adamberg, T. Visnapuu, T. Alamäe, Bacterial polysaccharide levan as stabilizing, non-toxic and functional coating material for microelement-nanoparticles, *Carbohydrate Polymers* 136 (2015) 710−720.
9. A. Šutka, M. Timusk, N. Döbelin, R. Pärna, **M. Visnapuu**, U. Joost, T. Käämbre, V. Kisand, K. Saal, M. Knite, A straightforward and "green" solvothermal synthesis of Al doped zinc oxide plasmonic nanocrystals and piezoresistive elastomer nanocomposite, *RSC Advances* 5 (2015) 63846−63852.

10. A. Ivask, T. Titma, **M. Visnapuu**, H. Vija, A. Käkinen, M. Sihtmäe, S. Pokhel, L. Madler, M. Heinlaan, V. Kisand, R. Shimmo, A. Kahru, Toxicity of 11 Metal Oxide Nanoparticles to Three Mammalian Cell Types In Vitro, *Current Topics in Medicinal Chemistry* 15 (2015), 1914−1929.
11. A. Ivask, I. Kurvet, K. Kasemets, I. Blinova, V. Aruoja, S. Suppi, H. Vija, A. Käkinen, T. Titma, M. Heinlaan, **M. Visnapuu**, D. Koller, V. Kisand, A. Kahru, Size-dependent Toxicity of Silver Nanoparticles to Bacteria, Yeast, Algae, Crustaceans and Mammalian Cells in Vitro, *PLOS ONE* 9 (2014) e102108.
12. U. Joost, A. Saarva, **M. Visnapuu**, E. Nõmmiste, K. Utt, R. Saar, V. Kisand, Purification of titania nanoparticle thin films: Triviality or a challenge? *Ceramics International* 40 (2014), 7125−7132.
13. **M. Visnapuu**, U. Joost, K. Juganson, K. Künnis-Beres, A. Kahru, V. Kisand, A. Ivask, Dissolution of silver nanowires and nanospheres dictates their toxicity to *Escherichia coli*, *BioMed Research International* (2013) 819252.
14. U. Joost, R. Pärna, M. Lembinen, K. Utt, I. Kink, **M. Visnapuu**, V. Kisand, Heat treatment and substrate dependent properties of titania thin films with high copper loading, *Physica Status Solidi A – Applications and Materials Science* 210 (2013) 1201–1212.

DISSERTATIONES TECHNOLOGIAE UNIVERSITATIS TARTUENSIS

1. **Imre Mäger**. Characterization of cell-penetrating peptides: Assessment of cellular internalization kinetics, mechanisms and bioactivity. Tartu 2011, 132 p.
2. **Taavi Lehto**. Delivery of nucleic acids by cell-penetrating peptides: application in modulation of gene expression. Tartu 2011, 155 p.
3. **Hannes Luidalepp**. Studies on the antibiotic susceptibility of *Escherichia coli*. Tartu 2012, 111 p.
4. **Vahur Zadin**. Modelling the 3D-microbattery. Tartu 2012, 149 p.
5. **Janno Torop**. Carbide-derived carbon-based electromechanical actuators. Tartu 2012, 113 p.
6. **Julia Suhorutšenko**. Cell-penetrating peptides: cytotoxicity, immunogenicity and application for tumor targeting. Tartu 2012, 139 p.
7. **Viktoryia Shyp**. G nucleotide regulation of translational GTPases and the stringent response factor RelA. Tartu 2012, 105 p.
8. **Mardo Kõivomägi**. Studies on the substrate specificity and multisite phosphorylation mechanisms of cyclin-dependent kinase Cdk1 in *Saccharomyces cerevisiae*. Tartu, 2013, 157 p.
9. **Liis Karo-Astover**. Studies on the Semliki Forest virus replicase protein nsP1. Tartu, 2013, 113 p.
10. **Piret Arukuusk**. NickFects–novel cell-penetrating peptides. Design and uptake mechanism. Tartu, 2013, 124 p.
11. **Piret Villo**. Synthesis of acetogenin analogues. Asymmetric transfer hydrogenation coupled with dynamic kinetic resolution of α-amido-β-keto esters. Tartu, 2013, 151 p.
12. **Villu Kasari**. Bacterial toxin-antitoxin systems: transcriptional cross-activation and characterization of a novel *mqsRA* system. Tartu, 2013, 108 p.
13. **Margus Varjak**. Functional analysis of viral and host components of alphavirus replicase complexes. Tartu, 2013, 151 p.
14. **Liane Viru**. Development and analysis of novel alphavirus-based multifunctional gene therapy and expression systems. Tartu, 2013, 113 p.
15. **Kent Langel**. Cell-penetrating peptide mechanism studies: from peptides to cargo delivery. Tartu, 2014, 115 p.
16. **Rauno Temmer**. Electrochemistry and novel applications of chemically synthesized conductive polymer electrodes. Tartu, 2014, 206 p.
17. **Indrek Must**. Ionic and capacitive electroactive laminates with carbonaceous electrodes as sensors and energy harvesters. Tartu, 2014, 133 p.
18. **Veiko Voolaid**. Aquatic environment: primary reservoir, link, or sink of antibiotic resistance? Tartu, 2014, 79 p.
19. **Kristiina Laanemets**. The role of SLAC1 anion channel and its upstream regulators in stomatal opening and closure of *Arabidopsis thaliana.* Tartu, 2015, 115 p.

20. **Kalle Pärn**. Studies on inducible alphavirus-based antitumour strategy mediated by site-specific delivery with activatable cell-penetrating peptides. Tartu, 2015, 139 p.
21. **Anastasia Selyutina**. When biologist meets chemist: a search for HIV-1 inhibitors. Tartu, 2015, 172 p.
22. **Sirle Saul**. Towards understanding the neurovirulence of Semliki Forest virus. Tartu, 2015, 136 p.
23. **Marit Orav**. Study of the initial amplification of the human papillomavirus genome. Tartu, 2015, 132 p.
24. **Tormi Reinson**. Studies on the Genome Replication of Human Papillomaviruses. Tartu, 2016, 110 p.
25. **Mart Ustav Jr**. Molecular Studies of HPV-18 Genome Segregation and Stable Replication. Tartu, 2016, 152 p.
26. **Margit Mutso**. Different Approaches to Counteracting Hepatitis C Virus and Chikungunya Virus Infections. Tartu, 2016, 184 p.
27. **Jelizaveta Geimanen**. Study of the Papillomavirus Genome Replication and Segregation. Tartu, 2016, 168 p.
28. **Mart Toots**. Novel Means to Target Human Papillomavirus Infection. Tartu, 2016, 173 p.
29. **Kadi-Liis Veiman**. Development of cell-penetrating peptides for gene delivery: from transfection in cell cultures to induction of gene expression *in vivo*. Tartu, 2016, 136 p.
30. **Ly Pärnaste**. How, why, what and where: Mechanisms behind CPP/cargo nanocomplexes. Tartu, 2016, 147 p.
31. **Age Utt**. Role of alphavirus replicase in viral RNA synthesis, virus-induced cytotoxicity and recognition of viral infections in host cells. Tartu, 2016, 183 p.
32. **Veiko Vunder**. Modeling and characterization of back-relaxation of ionic electroactive polymer actuators. Tartu, 2016, 154 p.
33. **Piia Kivipõld**. Studies on the Role of Papillomavirus E2 Proteins in Virus DNA Replication. Tartu, 2016, 118 p.
34. **Liina Jakobson**. The roles of abscisic acid, CO_2, and the cuticle in the regulation of plant transpiration. Tartu, 2017, 162 p.
35. **Helen Isok-Paas**. Viral-host interactions in the life cycle of human papillomaviruses. Tartu, 2017, 158 p.
36. **Hanna Hõrak**. Identification of key regulators of stomatal CO_2 signalling via O_3-sensitivity. Tartu, 2017, 260 p.
37. **Jekaterina Jevtuševskaja**. Application of isothermal amplification methods for detection of *Chlamydia trachomatis* directly from biological samples. Tartu, 2017, 96 p.
38. **Ülar Allas.** Ribosome-targeting antibiotics and mechanisms of antibiotic resistance. Tartu, 2017, 152 p.
39. **Anton Paier.** Ribosome Degradation in Living Bacteria. Tartu, 2017, 108 p.
40. **Vallo Varik.** Stringent Response in Bacterial Growth and Survival. Tartu, 2017, 101 p.

41. **Pavel Kudrin.** In search for the inhibitors of *Escherichia coli* stringent response factor RelA. Tartu, 2017, 138 p.
42. **Liisi Henno.** Study of the human papillomavirus genome replication and oligomer generation. Tartu, 2017, 144 p.
43. **Katrin Krõlov.** Nucleic acid amplification from crude clinical samples exemplified by *Chlamydia trachomatis* detection in urine. Tartu, 2018, 118 p.
44. **Eve Sankovski.** Studies on papillomavirus transcription and regulatory protein E2. Tartu, 2018, 113 p.
45. **Morteza Daneshmand.** Realistic 3D Virtual Fitting Room. Tartu, 2018, 233 p.
46. **Fatemeh Noroozi.** Multimodal Emotion Recognition Based Human-Robot Interaction Enhancement. Tartu, 2018, 113 p.
47. **Krista Freimann.** Design of peptide-based vector for nucleic acid delivery in vivo. Tartu, 2018, 103 p.
48. **Rainis Venta.** Studies on signal processing by multisite phosphorylation pathways of the *S. cerevisiae* cyclin-dependent kinase inhibitor Sic1. Tartu, 2018, 155 p.
49. **Inga Põldsalu.** Soft actuators with ink-jet printed electrodes. Tartu, 2018, 85 p.
50. **Kadri Künnapuu**. Modification of the cell-penetrating peptide PepFect14 for targeted tumor gene delivery and reduced toxicity. Tartu, 2018, 114 p.
51. **Toomas Mets**. RNA fragmentation by MazF and MqsR toxins of *Escherichia coli.* Tartu, 2019, 119 p.
52. **Kadri Tõldsepp**. The role of mitogen-activated protein kinases MPK4 and MPK12 in CO_2-induced stomatal movements. Tartu, 2019, 259 p.
53. **Pirko Jalakas**. Unravelling signalling pathways contributing to stomatal conductance and responsiveness. Tartu, 2019, 120 p.
54. **S. Sunjai Nakshatharan**. Electromechanical modelling and control of ionic electroactive polymer actuators. Tartu, 2019, 165 p.
55. **Eva-Maria Tombak**. Molecular studies of the initial amplification of the oncogenic human papillomavirus and closely related nonhuman primate papillomavirus genomes. Tartu, 2019, 150 p.